CIVIL ENGINEERING STUDIES

STRUCTURAL RESEARCH SERIES NO. 198

THE EFFECT OF COOLING RATE AND RESTRAINT ON WELD CRACKING

By
W. L. JOHNSON
and
J. E. STALLMEYER

A TECHNICAL REPORT
OF A RESEARCH PROGRAM
Sponsored by the
CHICAGO BRIDGE & IRON COMPANY

UNIVERSITY OF ILLINOIS
URBANA, ILLINOIS
JUNE 1961

THE EFFECT OF COOLING RATE AND RESTRAINT ON WELD CRACKING

by

W. L. Johnson and J. E. Stallmeyer

A Technical Report

Of a Research Program

Sponsored by the

CHICAGO BRIDGE & IRON COMPANY

University of Illinois

Urbana, Illinois

June 1961

TABLE OF CONTENTS

LIST OF TABLES

LIST OF FIGURES

LIST OF FIGURES

LIST OF FIGURES (Continued)

Figure Number

PART A: A STUDY OF WELD CRACKING AS A FUNCTION OF COOLING RATES

I. INTRODUCTION

1. Object and Scope of Investigation

It is well known that peak temperatures and cooling rates that occur during welding have a definite effect on the metallurgical structure and properties of the weld metal and material being welded. Peak temperatures will determine the constituents that will be formed as a result of heating, while the transformation products formed during cooling are dependent upon the cooling rate. Both are important in welding, but in Part A of this paper the cooling rate is given major consideration.

The cooling rate is known to be a function of the energy input, joint geometry, and to some extent, the ambient temperature. In an attempt to keep the number of variables at minimum, only one type of steel and one type of electrode will be considered. The most common structural steel is ASTM designation A-7 steel and a widely used all-position electrode is the E-6010 electrode; therefore, this electrode-steel combination was chosen for the investigation.

Joint geometry is an important factor not only from the viewpoint of cooling rate, but also because of the degree of restraint that it imposes upon the weld metal during and after welding. According to a report published by C. L. M. Cottrell,(1) restraint is not necessary for the initiation of cracking but tends to amplify cracks initiated by other means. On this premise, fillet welds were investigated under Part A of this program. The fact that minimum fillet size requirements in the AWS specifications are based wholly on past experience and not on experimental data gives additional purpose to this investigation.

---

(1) Refers to reference listed in bibliography.

2. Discussion of Problem

Weld cracking can generally be of two major types: (a) high temperature or hot cracks that occur almost immediately upon or during solidification of the weld metal, and (b) low temperature or cold cracks that can occur either soon or possibly a day or two after welding. These two classifications of weld cracking are further discussed below.

(a) Hot cracks generally occur in root passes of fillet welds and are formed during solidification of the weld metal due to multiaxial tensile stresses induced by shrinkage due to cooling. Most hot cracks are of considerable magnitude and once initiated can propagate the entire length of the weld. A second type of hot crack, but somewhat less common, is cracking that initiates at and propagates along grain boundaries. The grain boundaries present a plane of weakness to the multiaxial tensile stresses that occur during solidification. It has been suggested[5] that hydrogen is a factor that contributes to hot cracking, however, the exact role of hydrogen is not understood but is believed to be instrumental.[2][3]

(b) Cold cracks are generally thought of as microcracks or underbead cracks. According to Flanigan,[3] the effect of hydrogen on microcracking is significant at low-temperature cooling rates but its effect is not clearly understood. The theory suggested by some investigators[4][5] of the role of hydrogen is as follows: During welding, quantities of hydrogen are dissolved into the weld metal and thereby can diffuse into the parent metal. Hydrogen is very soluble in austenite at all temperatures but is practically insoluble in cold ferrite or martensite. As a result, hydrogen is rejected upon cooling from all areas as the austenite transforms. The hydrogen can gather at any discontinuity in the form of molecular hydrogen and thereby build up pressures that may exceed the strength of the parent material and cause cracking.

The rate of cooling, as affected by joint geometry and energy input, is believed to be the most important factor associated with cold cracking while restraint is believed to be one of the most important factors associated with hot cracking. The high temperature cooling rate can be important since, when the cooling rate is at a low value, there will be sufficient time for hydrogen or other entrapped gases to diffuse to the surface, thus avoiding possible cracking due to these gases. The cooling rate at lower temperatures is significant as the transformation products are dependent upon the cooling rate. The role of restraint is somewhat debatable as can be seen from reports by various investigators who have used the cruciform[6][7] type test and those who have used the controlled thermal severity[1] test.

3. Acknowledgment

This investigation is a part of the structural research program conducted in the Civil Engineering Department at the University of Illinois under the direction of Dr. N. M. Newmark, Head of the Civil Engineering Department. Funds for this program have been provided by the Chicago Bridge and Iron Foundation, and the investigation was conducted by Wayne L. Johnson, the Chicago Bridge and Iron Research Assistant in Civil Engineering working under the direction of J. E. Stallmeyer, Professor of Civil Engineering. A considerable amount of the preliminary work was completed by Mr. R. S. Wozniak, and this preliminary study is acknowledged.

The author would like to express his appreciation to the Chicago Bridge and Iron Foundation for their support of his assistantship and the personnel of the Civil Engineering Department shop for their assistance. Considerable advice was given the author concerning the metallurgy of welding by Professor W. H. Bruckner of the Department of Metallurgy and this advice is very much appreciated.

II. EQUIPMENT

1. Test Specimen

In order to reduce the number of variables involved in welding, only one type of electrode and one type of steel was used. The electrode was the E-6010 all-position, D.C. reversed polarity electrode and the steel was an ASTM designation A-7 steel.

Cottrell, etal,[1] found that the volume of the test specimen could be considered a variable that affects the cooling rate of a weld. Small specimens can become completely heated above the ambient temperature and thereby reduce the cooling rate of the weld. This phenomenon is termed heat saturation from lack of an adequate heat sink. In order to preclude the possibility of heat saturation, a relatively large specimen should be used. The specimens used in this investigation exceed the minimum requirement for volume as prescribed by Cottrell.

Plate thickness is also an important variable up to the thickness at which the heat flow changes from two-dimensional flow to three-dimensional flow. Once three-dimensional heat flow exists for the given welding conditions, the cooling rate becomes independent of plate thickness and depends on energy input only; thus when three-dimensional heat flow exists, the cooling rate is approximately the same as it would be for an infinitely thick plate.

The specimen used for this study is made up of two plates of equal thickness, the bottom plate being 9 x 9-in. and the top 3 x 9-in. (see Fig. 1). Specimens with different thicknesses were used so that the effect of plate thickness on cooling rate could be studied. In order to measure the cooling rates in the heat-affected zone, thermocouples were inserted into holes of

predetermined depth drilled from the under side of the plate into the heat-affected zone.

2. Thermocouples

Chromel-alumel thermocouples for the measurement of heat-affected zone temperatures were fused together with a resistance welder which was modified for this purpose. The junction to be fused was hammered flat before welding. The thermocouples were then coated with "sauereisen", a commercial ceramic which acted as an insulator against stray currents during welding; however, this was found to be unnecessary and perhaps better values could have been recorded had the thermocouple junction been fused to the specimen itself.

The required hole depth for locating the thermocouple in the heat-affected zones had been determined by depositing preliminary welds which were sectioned and the depths of the heat-affected zones measured. The thermocouples were then located at the expected location of the heat-affected zone; however, variations in the depth of penetration proved to be greater than predicted. As a result, many of the thermocouple junctions were either consumed by the molten metal of the weld or were located at a distance too far from the fusion line to give results that could be considered reliable. Satisfactory results were obtained only from thermocouples that were located exactly at the fusion line. The number of measured cooling rates listed in Table 1 is indicative of the problem encountered. The measured cooling rates are to be used only as an indication of the validity of theoretically calculated cooling rates as will be shown later; therefore, extreme accuracy was not essential.

3. Welding Equipment

Welding was done manually and every effort made to duplicate typical shop welding procedures. If automatic welding equipment had been used utilizing high travel speed and high energy input, special consideration would have to be given to these effects.(8)(9)

The welding current was supplied by a 200 amp capacity Westinghouse D.C., type RA, welding machine. The electrodes were kept in a drying oven at a temperature of 300 deg. F. for several weeks prior to use in order to insure removal of moisture which might have been detrimental.

All specimens (See Fig. 3) were welded at room temperature (70 deg.-80 deg. F.); the second weld was not deposited until the specimen had returned to room temperature. During welding a recording oscillograph was used to record the voltage and amperage and the thermal history of the heat-affected zone. Calibration of the voltage and amperage traces had been made by applying the welding machine current to a salt-brine solution. The voltage was measured between the electrode holder and the ground clamp. The voltage and amperage were not constant during welding because of the changing arc length; therefore, the traces recorded on the oscillograph deviated by as much as 10 percent. An average value was taken in order to evaluate the energy input. (See Fig. 6)

4. Recording Oscillograph

The recording oscillograph was a Heiland Magnetic Oscillograph (Type SE-303R-12) modified for this application (See Fig. 2). This unit has 12 recording channels, five of which were used in the tests; two were held in reserve and the remaining channels were blocked out. The galvanometers were type A units (D.C. sensitivity, 800 MM/MA undamped).

The oscillograph and thermocouple galvanometers were calibrated with a standard millivolt source which simulated temperatures up to 2000 deg. F. A

study of the calibration curves showed a maximum error from average at 2000 deg. F. of 30° or $\pm$ 1 1/2%, an error which decreased linearly as the temperature decreased.

The motor speed driving the recording paper of the oscillograph was not constant; therefore, it was necessary to record the welding time for each test.

III. CRACK INVESTIGATION

Some longitudinal cracks could be observed by visual inspection; however, to determine positively whether or not a weld had cracked a magnetic particle inspection was utilized. A set of portable magnaflux prods (See Fig. 4) was used with a Lincoln, 600 amp, motor generator unit, utilizing a current of 100 amps/inch of distance between prods. A crack detected by this method is shown in Fig. 5.

The longitudinal type cracking encountered always occurred in the second fillet weld deposited and initiated at the terminal end of the weld. In general, the cooling rates measured at this location were higher than those measured at the center of the length of the weld. This is to be expected, however, as steady state conditions do not exist at either end of a weld. The terminal end of the weld also exhibited the characteristic crater caused by removal of the electrode with a resulting depression in the weld metal.

A decrease in weld metal area, the high cooling rate and restraint imposed by weld No. 1 can all be factors causing initiation of longitudinal weld metal cracking. The exact cause is unknown, but restraint seems to be the most important variable as only weld No. 2 exhibited this type of cracking.

Building up of weld metal at the terminal end by crater filling is recommended for two reasons. One, the cooling rate will be reduced as a result of the added energy input, and two, the added weld metal will add to the resistance to stresses due to shrinkage and thereby help prevent cracking.

It will be shown below that the elimination of microcracking encountered also tends to eliminate longitudinal type cracking.

Investigations conducted by Flanigan[3][11][12] using an E-6010 electrode and mild steel combination show the existence of microcracks in the weld metal. It was, therefore, assumed that this type of cracking would be encountered in this investigation. Also there is a report published by C. M. Adams[8] which makes it possible to calculate peak temperatures and cooling rates that occur during welding. The measured cooling rates were determined by constructing the slope of the time-temperature curve (See Fig. 6) at the temperature for which the cooling rate is desired. The cooling rates as measured by thermocouple No. 7, which is the thermocouple located at the center of the length of the weld, are shown in Table 1 and these values are also plotted on Fig. 16. The cooling rate for each specimen was calculated by use of Adams' equations and then, using these cooling rates as a basis for the order of examination, the welds in the order of decreasing cooling rates were examined for microcracks. (See Table 1.)

At mid-length of the weld, a section was removed which was approximately one inch long. This section was then cut at a 45 deg. angle through the throat of the weld. (See Fig. 7 for the polished specimen.) The section was then polished and etched using a 5 percent nitric acid, 95 percent ethyl alcohol etchant. Prior to etching, the specimen was examined under the microscope for cracking. This was done to preclude the possibility that any cracking found could have been caused by the etchant itself. After etching, the specimen was re-examined. If cracking was found to exist in the specimen, it was always found before etching, and if there was any additional cracking caused by etching, it was not discernible.

When cracking was found in one specimen, the specimen with the next lower calculated cooling rate was cut, polished, etched, and examined. This procedure was continued until specimens were found that had absolutely no cracking. In addition to the specimens that were welded and allowed to cool in still air at room temperature, one additional specimen (D-12-1) was welded and treated as follows. The first weld was laid and quenched in water at 70 deg. F. immediately after welding. The second weld was laid and then allowed to cool in still air with an ambient temperature of 20 deg. F. This was done to provide specimens with cooling rates other than would ordinarily occur.

From the specimens that were examined, five were selected on the basis of cooling rate and degree of cracking to be photomicrographed. These photomicrographs are shown in Figs. 9 through 13. Hardness surveys of each specimen were taken and the results are shown on Fig. 14.

IV. DETERMINATION OF COOLING RATES

During the preliminary phase of this investigation, many welds were laid during which the voltage and amperage was recorded. The fillet welds laid were sectioned and the leg lengths of the fillets were measured. A plot of leg lengths versus energy input in Joules per inch revealed that the relationship was approximately linear. The following equation was derived from this relationship: (See Fig. 15)

$$E.I. = 2.143 \times 10^5 (L - .094) \qquad (1)$$

where E.I. = energy input per inch (Joules per inch)

L = fillet leg length (inches)

This equation is very similar to one found by Cottrell[1] his equation being;

$$E.I. = 2 \times 10^5 (L - 0.09) \qquad (2)$$

This tends to bear out the fact that fillet welds deposited by A.C. current, which Cottrell used, and those deposited using D.C. reversed polarity are a linear function of the energy used to deposit the welds and are likewise quite independent of electrode coating.[1] Observation of the graph of Fig. 15 shows that Equation (1) (D.C. Reversed Polarity) will require higher energy inputs for larger welds, but approaches the A.C. values for smaller welds.

Generally, the values of energy input calculated by use of either Equation (1) or (2) would be adequate because there is considerable scatter of the plotted values. There is some question regarding the merits of inferred accuracy of Equation (1); however, Fig. 15 indicates that Equation (2) falls somewhat below the plotted data particularly at high energy inputs.

For 1/8-in. fillet welds either equation would give values that are too low. Better values can be obtained by using a curve as shown in Fig. 15 for values of energy input less than 20,000 Joules per inch. This situation occurs because the curve must pass through the origin. The equation used at higher energy inputs should be selected according to the current and polarity being used. (The relationship for D.C. straight polarity is not known at this time.)

Using either Equation (1) or (2), it is possible to determine the approximate energy input required to deposit a given size fillet. Knowing the fillet size desired and electrode to be used, we can then utilize the electrode manufacturers' recommended voltage and amperage to calculate the travel speed that will be necessary to deposit the desired size fillet.

Example: 5/16" fillet desired

From Fig. 15, 47,000 Joules/inch required.

Using A. O. Smith electrode chart:

Electrode 3/16"
Recommended current 170-190 (Flat position)
Recommended voltage 27-29

$$\frac{\text{Joules}}{\text{inch}} = \frac{VIt}{L} \text{ or Travel Speed } \left(\frac{\text{In.}}{\text{Min.}}\right) = \frac{\text{Voltage x Amperage}}{\text{Joules/inch}} \times 60$$

$$\text{Travel Speed} = \left(\frac{\text{In.}}{\text{Min.}}\right) = v = \frac{(170)(27)(60)}{(47{,}000)} = 5.86 \text{ In./Min. Minimum}$$

or

$$\text{Travel Speed} = \left(\frac{\text{In.}}{\text{Min.}}\right) = v = \frac{(190)(29)(60)}{(47{,}000)} = 7.04 \text{ In./Min. Maximum}$$

See Table 2 for minimum and maximum travel speeds to be used with the designated electrode size and fillet size. Similar relationships can be established for other electrode-fillet sizes or welding positions other than flat.

Once the required travel speed has been calculated, it becomes possible to calculate peak temperatures and cooling rates by the use of

equations developed by C. M. Adams.[8] Consideration must be given to the fact that a condition in which three-dimensional heat flow might exist could be changed to two-dimensional heat flow by varying travel speed and greatly increasing energy input. As a result of this possibility, peak temperatures and cooling rates must be calculated for both two- and three-dimensional heat flow. In the case of peak temperature, the highest value would be the more nearly correct while for cooling rate, the lower value would be the more correct.[8]

Peak temperatures:

2-dimensional heat flow

$$\frac{1}{T_p - T_o} = \frac{vr' t \rho C_p \sqrt{2\pi e}}{q} + \frac{1}{T_m - T_o} \qquad (3)$$

3-dimensional heat flow

$$\frac{1}{T_p - T_o} = \frac{2\pi K \alpha e}{qv} \left[2 + \left(\frac{vr'}{2\alpha} \right)^2 \right] + \frac{1}{T_m - T_o} \qquad (4)$$

Cooling Rates:

2-dimensional heat flow

$$C.R. = 2\pi K \rho C_p \left(\frac{vt}{q} \right)^2 (T' - T_o)^3 \qquad (5)$$

3-dimensional heat flow

$$C.R. = 2\pi K \frac{v}{q} (T' - T_o)^2 \qquad (6)$$

where:

T_p = peak temperature ($^{\circ}F.$)

T_o = plate temperature ($^{\circ}F.$)

K = thermal conductivity of plate (Btu/ft.-hr.$^{\circ}$F.)

v = velocity of source (In./Min.)

ρ = density of plate (Lbs./ft.^{3})

C_p = specific heat of plate (.155 Btu/lb.-$^{\circ}$F.)

t = plate thickness in inches

r' = distance from fusion line in inches

q = rate of heat flow from source (Btu/hr.)

T_m = melting temperature of metal ($^{\circ}$F.)

T' = temperature at which cooling rate desired

$\alpha = \frac{K}{\rho C_p}$

The value of K varies considerably but average values give fair results. For calculating peak temperatures K = 20 Btu/ft.-hr.-$^{\circ}$F. For calculating cooling rates

at 1000°F. $K \cong 22$ Btu/ft.-hr.-$^{\circ}$F.

at 750°F. $K \cong 24$ Btu/ft.-hr.-$^{\circ}$F.

at 572°F. $K \cong 26$ Btu/ft.-hr.-$^{\circ}$F.

The rate of heat flow for fillet welds for trithermal conditions is taken at 2/3 q and generally at 80 percent efficiency.(8)

In the previous discussion a method for calculating peak temperatures and cooling rates has been presented, this method can be used providing the thickness of the material to be welded is known. The plate thickness as used for fillet welds assumes that the top plate and bottom plates are of the same thickness. Should the top plate thickness vary from the bottom plate, consideration must be given to this variation if the conditions are such that two-dimensional heat flow governs. When the top plate thickness is relatively thin as compared to the bottom plate, then the rate of heat flow should be

taken at some value larger than 2/3 q. When the top plate is relatively thick as compared to the bottom plate, then the rate of heat flow should be taken somewhat less than 2/3 q. If three-dimensional heat flow governs, then the plate thickness has a negligible effect unless the top plate is relatively thin (1/2" or less). When this occurs the rate of heat flow should be increased somewhat above the 2/3 q value assumed. An alternate approach would be to adjust the heat flow efficiency accordingly.

V. CORRELATION OF THEORETICAL DATA AND CRACKING

In order to make use of any theoretically calculated cooling rates, it is necessary to establish a relationship between cooling rate and cracking. This has been done in the experimental phase of this investigation. Table 1 of this report shows the specimens that were welded, the energy inputs, the calculated cooling rates, and the measured cooling rates. The cooling rates are those occurring at 750 deg. F. since this is approximately the M_s temperature for mild steel and was calculated by using the M_s formula as presented in the Metals Handbook.(10)

Study of Table 1 shows that in all cases except when welding the 1/2-in. plate, the three-dimensional heat flow governed (lowest values). This would tend to indicate that under ordinary manual welding procedures, the heat flow will ordinarily be three-dimensional unless welding 1/2-in. or thinner plates. It is possible, however, to have two-dimensional heat flow govern whenever large energy inputs are used even on thicker plates. A plot of energy input versus cooling rate is shown in Fig. 16.

Micro-inspection of the specimens that were etched and polished shows that by using the cooling rate as a parameter, a cooling rate of 110 deg. F./sec. at 750 deg. F. can be taken as the dividing line between specimens that showed cracking and those that showed no cracking. Inspection of Table 1 shows that possibly a range of cooling rates should be considered as a range in which cracking might or might not occur. This is shown by specimen B-12-1, weld No. 1, in which no cracking occurred but for which the calculated cooling rate was 117 deg. F./sec. while specimen B-1-1, weld No. 2, which had a calculated cooling rate of 112 deg. F./sec., showed cracking. This difference might be attributed to the change in restraint introduced

because of variation in plate thickness. However, the cracks that existed were relatively minute as compared to the cracking shown in Fig. 18. The specimens inspected with cooling rates less than 110 deg. F./sec. showed no cracking; therefore, 110 deg. F./sec. is the approximate upper limit at which no cracking will occur. This becomes the critical cooling rate for the electrode plate combination investigated using the test configuration shown in Fig. 1.

It is also interesting to note that the smallest longitudinal crack (Fig. 5) occurred at the corresponding cooling rate of 112 deg. F./sec. and in the same weld in which the smallest (Fig. 18) type crack was found (See Table 1). With reduced cooling rates Fig. 5 type cracking was no longer encountered. It is possible that the two types of cracking are dependent upon cooling rate, although the role of restraint would have to be investigated further by varying the test specimen configuration and noting the effect on the longitudinal type cracking. It must be remembered, however, that the longitudinal crack was initiated at the terminal end of the weld where different thermal conditions exist and a cooling rate greater than 112 deg. F./sec existed.

Another observation from Table 1 shows that the specimen D-12-1, weld No. 1 which was quenched, exhibited only 1 crack/inch and this was relatively small. The cooling rate was definitely the most severe and the only explanation available for the lack of cracking is as explained in a paper by Flanigan and Saperstein[12] which states that a brief period of immunization to cracking prevails after welding. If quenched during this period the welds will show little, if any, microcracking.

The solid curve of Fig. 16 was plotted using only the values for cooling rates as determined by Equation (6) which is for three-dimensional heat flow. Superimposed upon Fig. 16 are the cooling rates as calculated by use of Equation (5) for two-dimensional heat flow. Although there was insufficient measured data available to plot completely the two-dimensional heat flow curves, additional data was calculated using Equation (1) and the recommended voltages and amperages.

The significance of plotting both two- and three-dimensional heat flow cooling rate curves is as follows. The intercept of a two-dimensional heat flow curve with the three-dimensional curve is the transition point. Above the intercept two-dimensional heat flow governs (Equation 5). Below the intercept three-dimensional heat flow governs (Equation 6). Calculating the energy input/inch by use of Equation (1) allows one to enter Fig. 16 directly and the cooling rate can readily be determined providing the plate thickness is known. (Top and bottom plate thicknesses are equal for curves on Fig. 16).

For example, suppose it is necessary to deposit a 5/16-in. fillet weld on 3/4-in. plate (top and bottom plates 3/4-in. thick). From Fig. 15 it is noted that this fillet requires approximately 47,000 Joules/inch energy input. Entering Fig. 16 at 47,000 Joules/inch, one finds that for the 3/4-in. plate two-dimensional heat flow gives the lowest cooling rate value and, therefore, governs. (Note that we are above the intercept of the two- and three-dimensional heat flow curves for 3/4-in. plate.) The corresponding cooling rate is approximately 50 deg. F./sec. and considerably below the critical cooling rate of 110 deg. F. Therefore, no cracking will be encountered. Now assume that it is necessary to lay a 3/16-in. fillet weld on the same plate. This requires approximately 20,000 Joules/inch (Fig. 15).

Entering Fig. 16 again at 20,000 Joules/inch one finds that this point is below the intercept of the two- and three-dimensional heat flow curves and, therefore, the three-dimensional heat flow governs. The corresponding cooling rate would be approximately 160 deg. F./sec., which is above the critical cooling rate of 110 deg. F./sec. and consequently a 3/16-in. weld should not be deposited on 3/4-in. plate. However, preheat could be used to reduce the cooling rate so that the 3/16-in. weld could be used. The amount of preheat can be determined from Equations (5) and (6) by substituting 110 deg. F./sec. for the cooling rate and solving for T_o, the plate temperature. Tests using preheat have not been run to date so this method of determining the amount of preheat should be used with caution.

Also plotted on Fig. 16 are the cooling rates which were measured at 750 deg. F. by the thermocouples which were inserted into the heat-affected zone at mid-length of the weld. The locations of the points indicate that the calculated cooling rates are somewhat lower than the measured values. This is true more so at low energy input values than for high values. The calculated values are for cooling rates that occur at the center of the weld bead while those measured occur at a point in the heat-affected zone. Theoretically the cooling rates in the weld bead should be greater than those in the heat-affected zone. The discrepancy could be due to the selection of the value of K (thermal conductivity) which varies for different temperatures or to the assumed efficiency of heat flow. Additional testing might result in a better selection of K or efficiency of heat flow in order to adjust the theoretical curve to fit the measured values. The measured values for cooling rates should be taken in the weld bead itself for maximum agreement between theory and tests.

Inspection of Table 1 shows that only a small number of the measured cooling rate values are shown. It was found that, in a number of instances, the distance from the thermocouple junction to the fusion line was so great that relatively low peak temperatures were recorded. The cooling rate at 750 deg. F. occurred near the peak of the time-temperature curve (See Fig. 6); therefore, the values were of doubtful value and not included.

In addition to calculating the cooling rates at 750 deg. F., the cooling rates at 572 deg. F. (300 deg. C.) using K = 26 Btu/ft.-hr.-^{o}F. were calculated. These values are shown in Table 5 and are plotted on Fig. 17. The same general characteristics occur in both cases; however, a greater number of measured cooling rates are available at the lower temperature. It can be seen from Fig. 17 that the discrepancy between calculated and measured cooling rates is greater at 572 deg. F. than at 750 deg. F. This is partially due to the fact that the additional measured cooling rates plotted have a larger error because of a greater distance from the fusion line to the thermocouple location which resulted in lower peak temperatures being recorded. The peak temperature can be used as an indication of the weight which should be given to the measured cooling rates when they are compared with the calculated cooling rates. This is due to the fact that the calculated cooling rates are those that occur at the center line of the weld metal and this automatically assumes a peak temperature equal to that of the molten metal. On the other hand, any measured cooling rate outside the molten pool actually will have a peak temperature somewhat less than the temperature of the molten metal. The peak temperature will depend on the distance from the fusion line.

Inspection of Fig. 16 and Fig. 17 shows that, in general, there is fair agreement between calculated cooling rates and measured values. If

Table 5 is used to determine the critical cooling rate, it is found to be approximately 65 deg. F./sec. at 572 deg. F. However, it seems that the relationship between cooling rate and cracking is much better at 750 deg. F. than at 572 deg. F., also, there is a rational basis for choosing a cooling rate at 750 deg. F. as it is the approximate M_s temperature for mild steel. Therefore, the critical cooling rate of 110 deg. F./sec. at 750 deg. F. shall be used throughout Part A of this report.

VI. RELATIONSHIP OF COOLING RATE TO SPECIFICATIONS

The AWS welding specifications for fillet welds are based on experience only; therefore, it is desirable to determine whether or not the specifications are safe, unsafe, or too conservative. This can be done, at least for the electrode-plate combination as used in this report. Table 3 lists the minimum fillet size that is to be used with the given plate thicknesses according to specifications. Table 2 shows the energy input (Joules/inch) that would be required to deposit the given size fillet. This energy input was calculated by use of Equation (1). Table 2 also shows the minimum and maximum welding speeds that could be used to lay the designated fillet size with the electrode shown. This was calculated using

$$\frac{(\text{Volts})(\text{Amps})(60)}{\text{Joules/inch}} = v \text{ inches/min.}$$

Table 3 shows the plate thicknesses and minimum fillet sizes as designated by the specifications and the corresponding cooling rates calculated by use of Equations (5) and (6). By inspection of Table 3 it can be seen that all of the governing calculated cooling rates are somewhat less than the critical cooling rate of 110 deg. F./sec. except the cooling rate for a 3/16-in. fillet on 1/2-in. plate. This indicates that cracking might possibly occur in the 3/16-in. fillet. Therefore, a larger weld requiring a larger energy input/inch should be used on 1/2-in. plates. Equation (1) indicates that a 1/4-in. fillet requires 33,500 Joules/inch. Entering Fig. 16 one finds that the corresponding cooling rate for 3/4-in. plate is 92 deg. F./sec. and for thicker plates in which three-dimensional heat flow governs, 95 deg. F./sec. Therefore, a 1/4-in. fillet weld could be the minimum size fillet required for any plate thicknesses for this electrode-plate combination.

Table 4 shows the comparison of the specified fillet sizes and those recommended in this report and tends to show that the specifications are conservative for thick plates but are possibly unsafe for the 1/2-in. plate for this electrode-plate combination.

VII. INVESTIGATION OF MICROSTRUCTURE

Investigations conducted by Flanigan[3][11] using the E-6010 electrode and mild steel combination for welding have indicated the influence of hydrogen on cracking. Flanigan has also shown that reducing the cooling rate by use of preheat will reduce and possibly eliminate cracking. The results of the investigation reported herein also tend to show that a reduction in cooling rate will reduce or eliminate cracking.

It is well known that the transformation products, martensite, bainite, and pearlite, are dependent upon the cooling rate, and it seems that the diffusion rate of hydrogen is also dependent upon cooling rate. It would be desirable to know whether or not the transformation products can be related to the cracking encountered.

In an attempt to clarify the role of the transformation products, a series of specimens was examined at a magnification of 500. The severity and type of cracking, as well as the calculated cooling rates, of this series is shown in Table 1. Examination of Table 1 shows that generally the severity of cracking decreases with decreasing cooling rate. The micro-examination showed that the acicular martensitic type structure existed in varying degrees in specimens that had cooling rates below the critical cooling rate and in which no cracking was encountered.

The existence of the acicular type structure is also fairly evident in the series of photomicrographs Figs. 9 through 13. The magnitude and characteristics of the general type of cracking are shown in Figs. 18 through 20. The type of cracking shown in Fig. 21 (underbead crack), as well as that shown in Fig. 22, in which the crack propagated into the heat-affected zone occurred in only one specimen, and this is one that showed extreme hardness in the heat affected zone as will be shown by the hardness survey.

A hardness survey was taken of the specimens shown in Figs. 9 to 13 using a Tukon Hardness Tester (Model FB) with a 136° diamond pyramid and a 500 gram load. The results of the hardness survey are shown in Fig. 14. Study of Fig. 14 shows that a high degree of hardness occurred in the weld metal. Specimens 1, 2, and 3 had cracking in the weld metal while 4 and 5 did not. It is interesting to note that 4 had higher hardness than 3 in the weld metal but did not develop cracking. It is also interesting to note that the cracking shown in Figs. 21 and 22 occurred only in specimen 3 which exhibits extreme hardness in the heat-affected zone close to the fusion line. A comparison of hardness and cooling rate shows that the degree of microhardness does not necessarily decrease with decreasing cooling rate.

From the results obtained from the microhardness surveys it has been concluded that no suitable relationship between microhardness and microcracking can readily be established. Nor does it seem feasible to relate the transformation products to microcracking unless extensive tests are carried out to determine the existence of martensite, tempered martensite, or bainite, as the acicular-type microstructure common to these constituents was found to exist at cooling rates below the critical cooling rate.

VIII. SUMMARY AND CONCLUSIONS

The number of specimens that have been tested in this investigation are somewhat limited, but the following conclusions seem to be justified.

1. Results of plotting energy input (Joules/inch) versus fillet leg length show an approximate linear relationship exists for D.C. reversed polarity as well as for A.C. welds deposited manually using relatively low travel speeds and nominal voltage and amperage.

2. The travel speed required to lay a desired size fillet can be computed by using Equation (1) and the voltage and amperage recommended by the electrode manufacturer.

3. Peak temperatures and cooling rates can be calculated by use of equations developed by C. M. Adams.[8] Fair agreement between actual cooling rates and those calculated at 750 deg. F. can be shown. Whether two- or three-dimensional heat flow exists depends on plate thickness, energy input, and initial plate temperature; therefore, it is necessary to calculate cooling rates for both cases, the lower cooling rate being the more correct.[8]

4. The results of this investigation using the test configuration shown in Fig. 1 tend to show that a critical cooling rate was determined to be 110 deg. F./sec. at 750 deg. F. from the micro-inspection of all specimens. A further look at Table 1 will disclose that by separating the specimens into groups containing only specimens of the same thickness, a critical cooling rate for each thickness might be established. For example, Specimen B-12-1, Weld No. 1, with a cooling rate of 117 deg. F./sec. had no cracking while the specimen with the lowest cooling rate that had cracking (B-1-1, Weld No. 2) is twice as thick. This indicates that possibly a critical cooling rate exists for each plate thickness due to the variation in the stress conditions

imposed by the different plate thicknesses. Additional testing must be carried out to evaluate this possibility; however, use of the results as presented in this report would be conservative.

A critical cooling rate at temperatures other than at 750 deg. F. can also be determined as is shown by the critical cooling rate determined at 572 deg. F. (300 deg. C.) and shown on Fig. 17. However, the best correlation between cracking and cooling rates seems to occur at 750 deg. F., which is approximately the M_s temperature for mild steel.

5. The electrode-plate combination as used in this investigation showed considerable susceptibility to both microcracking in the weld metal and longitudinal cracking. From the calculated cooling rates as shown in Table 3, it can be seen that a 3/16-in. weld on 1/2-in. plate exceeds the critical cooling rate of 110 deg. F./sec. and, therefore, could possibly possess microcracks and/or longitudinal cracking.

The AWS specifications allow 3/16-in. fillet welds to be placed on 1/2-in. plates and are, therefore, possibly unsafe. For other minimum size fillet welds on thicker plates the AWS specifications are conservative.

6. Investigation of the microstructure seems to indicate that cracking is not necessarily associated with the transformation products as the acicular-type microstructure persisted in the heat-affected zone even after cracking had been eliminated. The specimen with the most severe cracking in the weld metal had the lowest hardness in the heat-affected zone. (See Fig. 14.) It would, therefore, seem that the transformation products cannot readily be used as a parameter for determining a critical cooling condition; however, it must be noted that extreme hardness in the

heat-affected zone can very well be detrimental, for it was found that cracks initiated in the weld metal can propagate into the base metal (See Fig. 14 and Fig. 22) and become more serious than would be the case if cracking were confined to the weld metal itself.

7. Observation of Fig. 5 and Fig. 18 through Fig. 20 shows the general type and magnitude of cracks encountered in this investigation. There is a possibility that restraint may affect the magnitude of the cracks, as well as the critical cooling rate as was noted under conclusion No. 4. However, this possibility remains to be investigated. Restraint definitely seems to be a factor that affects longitudinal cracking (Fig. 5) as longitudinal cracking occurred only in Weld No. 2 where additional lateral restraint is imposed by Weld No. 1. Under highly restrained conditions, it would be desirable to deposit an oversize fillet rather than one that would just meet critical cooling rate requirements. This would be desirable for the following reasons: all of the longitudinal cracks which were encountered had originated at the terminal end of the weld where a crater exists and the cooling rate is somewhat higher than that along the length of the weld. The crater has a reduction in weld metal area and, therefore, a reduction in resistance to weld metal cracking while the increased cooling rate might conceivably exceed the critical rate and, therefore, help to initiate cracking. Backstepping or any other method of crater filling will help to preclude the possibility of longitudinal cracking.

8. Quenching upon completion of a weld seems to eliminate or at least decrease the severity of cracking. Only one specimen was quenched in this investigation, but the results are in accord with results found by Flanigan.[12] The limiting time in which the weld must be quenched, however,

is unknown; therefore, this procedure cannot be recommended. The possibility that martensite will be formed is greatly increased by quenching. Should quenching be used to prevent microcracking, thermal treatment should be used to produce tempered martensite if service conditions demand a more ductile, impact-resistant product.

9. If welds must be laid under conditions in which the critical cooling rate might be exceeded, then preheat should be used. The use of preheat has been found to be more effective at reducing low temperature cooling rates than has postheat.[11] The amount of preheat required can be found by using the critical cooling rate in Equations (5) and (6) and solving for the required initial plate temperature T_o.

10. The method as used in this investigation for determining critical cooling rates, as well as the method used for calculating cooling rates, can be used for any other electrode-plate combination as long as nominal values of voltage, amperage, and travel speed are used such as would be expected in manual welding. The possibility that restraint might affect the critical cooling rate indicates that at present this type of analysis should be limited to conditions of nominal restraint only.

PART B: A STUDY OF THE EFFECT OF PLATE THICKNESS ON THE CRITICAL COOLING RATE OF WELDS

IX. INTRODUCTION

1. Introductory Statement

In the first phase of this program, reported in Part A of this report, it was determined that a critical cooling rate for welds does exist for an ASTM designation A-7 steel and the E-6010 electrode combination. A correlation was obtained between the cooling rate at 750 deg. F. and the presence of weld cracks. At 750 deg. F. a critical cooling rate was determined; above which microcracking in the weld metal occurred and below which no cracking occurred. The critical cooling rate for welds was determined from a series of test specimens on which fillet welds were deposited manually and then sectioned, polished, etched, and examined microscopically for cracks. The fillet welds were deposited on plates of different thicknesses, and one critical cooling rate was determined for the entire series. No attempt was made to determine the effect of restraint caused by geometry or plate thickness upon the critical cooling rate.

2. Object and Scope

From the results of the series of tests reported herein, an attempt is made to determine the effect of restraint upon the critical cooling rate; the restraint being taken as a function of plate thickness. The effect of restraint has been evaluated by determining a critical cooling rate for each plate thickness tested. It was necessary to deposit only bead-on-plate welds in order to study the role of restraint. In this way the effect of joint geometry has been eliminated and the study of

restraint simplified. The degree of restraint imposed upon a bead-on-plate weld is to a certain degree a function of the thickness of the plate being welded. This is readily understood when one considers the fact that welds on thin plates produce maximum distortion and, as a result, minimum residual stress, while thick plates produce minimum distortion and, as a result, maximum residual stress.

From the work reported in Part A it was noted that a different critical cooling rate might exist for each plate thickness tested. This possible difference in critical cooling rates was thought to be a function of the restraint imposed on the weld due to plate thickness. As a result, the series of tests reported herein is an attempt to clarify the role of restraint upon the critical cooling rate of welds. Restraint is taken as a function of the plate thickness, and no attempt is made to distinguish between thermal stresses, stresses due to specimen geometry, or stresses which result from volumetric changes due to phase transformations.

X. MATERIAL AND EQUIPMENT

1. Material

The material used in this investigation is similar to the material used in the study reported in Part A, namely, an ASTM designation A-7 steel in the as-rolled condition in combination with an E-6010 electrode.

Several tension tests were carried out using standard tensile specimens made from the 3/4-in. and 1 1/4-in. thick plates. A chemical analysis of representative samples from various plate thicknesses was also performed. These tests were conducted in order to further classify the material investigated. The results of these tests, as well as properties (manufacturer's values) of the electrodes used, are listed in Table 6.

2. Test Specimen

The specimens used in this investigation were 4 1/2 x 9-in. plates and varied in thickness from 3/8-in. to 1 1/2-in. (See Fig. 24) The size of the specimen was such that heat saturation did not occur during welding. According to Cottrell, the volume of an ideal weldability test assembly should be greater than 36-1/2 t cubic inches in order to avoid heat saturation.(1) This condition is satisfied by the test specimens used in this investigation. A 3/32-in. diameter hole was drilled through the test specimen and a steel plug of a predetermined thickness was inserted into the hole from the side to be welded. This was done only for the 3/8-in., 3/4-in., and 1 1/4-in. thick plates and was done to insure that the depth to the thermocouple would be known. For the 1/2-in. and 1 1/2-in. plates the thermocouple was inserted manually into the molten weld pool; therefore, no holes were required in these test specimens. After welding, a section approximately 1-in. long was removed from the mid-length of the weld (See Fig. 24) for polishing and subsequent microinspection for cracks.

3. Equipment

Welding was done using a Lincoln Ideal arc electric welding machine. A modified procedure using a semi-automatic welding method was utilized in place of manual welding. An Airco Radiograph machine with a travel speed control mechanism was adapted for this purpose. The manual electrode holder was mounted on a vertical movable shaft, allowing the electrode to be fed manually while the travel speed could be preset on the Airco Radiograph machine. (See Fig. 25 for a general view of the welding equipment.)

By controlling the travel speed and presetting the voltage and amperage of the welding machine, an approximate predetermined energy input per inch could be obtained. The cooling rate is a function of the energy input; therefore, it is a simple matter to obtain specimens with different cooling rates merely by varying the travel speed and holding the voltage, amperage, and plate thickness constant.

The cooling rates that occurred in the weld were measured by using chromel-alumel thermocouples encased in a 3/32-in. diameter ceramic thermocouple tube. The junction was coated with "sauereisen", a commercial ceramic paste which hardens upon drying and acts as an insulator. Recording of the cooling rates that occurred in the weld was accomplished initially by photographing on 35 mm film the beam of a Model 512 Tektronix oscilloscope. However, this method did not prove to be entirely satisfactory; therefore, an alternate method of recording the cooling rates was adopted. In place of the oscilloscope, a Leeds and Northrup Type G Speedomax recorder, 3/4 second, full deflection, was used. This recorder proved to have adequate sensitivity, was much simpler to operate, and did not involve development or enlargement of film.

XI. TEST PROCEDURE

In order to simplify the restraint, and therefore the role of stress, as much as possible, only bead-on-plate welds are considered in this series of tests. Stresses due to restraint, thermal stresses, and stresses due to volumetric changes are all considered using plate thickness as the parameter. The use of plate thickness as the parameter eliminates the necessity of measuring actual strains that do occur as a result of welding. However, measurement of residual strains would help to relate different test specimen configurations to one another. It was anticipated from the results of tests reported in Part A that stresses due to restraint would affect the critical cooling rate. The results of this investigation tend to bear out this conclusion and this effect can readily be seen from the plot of plate thickness vs. critical cooling rate. (See Fig. 23.)

Initially in this investigation only 1/2-in. and 1 1/2-in. thick plate specimens were welded. This was done primarily to determine whether or not a different critical cooling rate did exist for plates of different thicknesses. This was found to be the case as can be seen from Fig. 23 or Table 7; therefore, the additional plate thicknesses were investigated.

The procedure used to measure and record the cooling rates for the 1/2-in. and 1 1/2-in. plates was somewhat different from the procedure used for the 3/8-in., 3/4-in., and 1 1/4-in. plates and, therefore, shall be described first.

The welds were deposited in the flat position using the semi-automatic procedure described previously (See Fig. 25). The welding arc was ignited by using a small amount of steel wool. At the desired location along the length of the weld, the thermocouple, encased in the ceramic tube, was

inserted manually into the molten pool that exists just behind the welding arc. This method of injecting the thermocouple into the weld metal worked fairly well, and peak temperatures that were below that of the melting temperature of the thermocouple (2400 deg. F.+) could be recorded. However, in the majority of the tests the melting temperature of the thermocouple was exceeded and, as a result, no cooling rate could be measured.

In an attempt to overcome the difficulty encountered in recording the cooling rates for the welds laid on the 1/2-in. and 1 1/2-in. plates, the following alternate procedure was adopted. From preliminary welds that had been deposited and for which the energy input was known, a plot of energy input vs. depth of penetration was constructed. From this graph the penetration for each weld could be estimated. Holes were then drilled through each specimen at mid-length of the proposed weld. Into each hole was inserted a steel plug the length of which was the estimated depth of penetration. The thermocouples which were encased in a 3/32-in. diameter thermocouple tube and which had the junction coated with "sauereisen" were then inserted into the holes in the test specimens. Using this procedure the location of the thermocouple was known and was presumed to be in the heat-affected zone close to the fusion line after the weld was deposited. This procedure produced somewhat lower recorded peak temperatures than the previously mentioned method, but the probability that the thermocouple would be consumed by the molten metal was reduced and the number of successfully recorded cooling rates was increased.

The cooling rates for the welds deposited on the 3/8-in., 3/4-in., and 1 1/4-in. plates were measured using the alternate method described

above and were recorded using a Leeds and Northrup Type G Speedomax Recorder. The measured cooling rates were calculated by constructing the slope of the time-temperature curve at 750 deg. F.

Although the alternate method of measuring and recording cooling rates proved to be somewhat more efficient than the initial procedure, the method left much to be desired. The major difficulty encountered was in locating the thermocouple so that maximum peak temperatures could be recorded without consuming the thermocouple junction in the molten weld metal. The voltage and amperage could not be controlled accurately enough with the equipment available to insure that the weld penetration would be the same as predicted. As a result, not all of the measured cooling rates were considered to be of value.

During welding the voltage across the electrode holder and ground clamp was read at several intervals and an average value recorded. The current was also recorded at several time intervals and average values of current and voltage were used to compute the energy input. The welding speed was recorded by timing the duration of welding and measuring the length of the weld.

XII. CRACK INVESTIGATION

In order to insure that all possible cracking of the welded specimens had taken place, the specimens were stored for several days at room temperature before the crack investigation was begun. The following procedure was used for the detection of the cracking.

A section approximately 1-in. long was removed from the center portion of the weld. This was accomplished by using a high speed cut off wheel utilizing a coolant in order to keep the temperature below the recrystallization temperature. (See Fig. 24)

The specimens were then prepared for microinspection of the weld metal and heat-affected zone by mechanical polishing and etching. The etchant used was a solution of 95% ethyl alcohol and 5% nitric acid. The specimens were then subjected to a microscopic examination at a magnification of 500. Typical cracking which was encountered was generally confined to the weld metal but was found to vary in magnitude and crack density. In no instance was cracking found to extend to the weld surface. (See Figs. 26 through 33)

It is interesting to note the magnitude of cracking as it varied with plate thickness as well as with cooling rate. A greater number of photomicrographs are included from the 1 1/2-in. thick plate series than from the other series (Figs. 30 through 33), because the P-1 1/2 series was found to have the greatest variation in type of cracking encountered. The reasons for this variation cannot be readily explained.

Inspection of Fig. 28 shows a crack that has propagated into the heat-affected zone of the base metal. Specimen P-3/4-1 was the only specimen found that contained this type of cracking. This specimen also had the

greatest number of cracks per inch; however, only one other crack in this specimen propagated into the heat-affected zone. An acicular martensitic-type structure was found to exist in the heat-affected zone, but whether it was martensite, tempered martensite, or bainite was not determined.

In addition to the photomicrographs showing the cracking encountered, two additional photomicrographs, Fig. 34 and Fig. 35, were taken. These are included to show the general characteristics of the microstructure of the base metal in the heat-affected zone. The acicular martensitic-type structure is fairly evident in both figures. Figure 35 is included to show the magnitude of some of the inclusions encountered in the base metal. It becomes apparent upon comparison of Fig. 35 and Fig. 31 that base metal inclusions could very well be as detrimental to a structure as could some of the microcracks encountered as a result of welding.

The results of the micro examination of all of the welded specimens are listed in Table 7. Also listed in Table 7 are the corresponding cooling rates for each specimen. It can easily be seen that as the cooling rate at 750 deg. F. decreased, the microcracking encountered was reduced and eventually eliminated. This result was found to be true for all plate thicknesses tested except the P-1 1/2 series for which lower cooling rate specimens were not available. However, from the results of the other series it would be expected that at a cooling rate of approximately 55 deg. F./sec. no further cracking would be encountered.

XIII. ANALYSIS AND EXPERIMENTAL RESULTS

1. Analysis

A definite relationship seems to exist between the critical cooling rate at 750 deg. F. and microcracking. This relationship is found to vary depending on the degree of restraint imposed upon the weld metal. The following section is devoted to clarifying this relationship, and simultaneously, presenting the information in simple graphical form. An attempt is also made to relate the results of the bead-on-plate tests to the fillet weld tests conducted previously.

The measured cooling rates are to be used as an experimental check on the validity of the theoretical equations developed by C. M. Adams.[8] These are the same equations that were used to calculate the cooling rates for the previous investigation on fillet welds except for the following change. The rate of heat flow from the source (100 percent) was taken as 2/3q for fillet-type welds in which there exists three avenues of heat flow away from the weld. This is known as a trithermal condition,[1] while for bead-on-plate welds used in this investigation the rate of heat flow from the source (100 percent) is taken as q and the two avenues of heat flow away from the weld constitute a bithermal condition.

For both fillet welds and bead-on-plate welds the efficiency of the rate of heat flow from the source (q) has been taken at 80 percent. It seems logical that the efficiency of energy input for the fillet weld should be higher than that for a bead-on-plate type weld due to the proximity of the material around the arc. The arc would tend to heat more material in the case of the fillet weld than it would for the bead-on-plate weld. Some discrepancy can be seen to exist between the results obtained from the fillet

weld tests and those obtained from the bead-on-plate tests. This discrepancy would seem to be due to the percent efficiency of heat flow from the source used to evaluate the cooling rates in each case. An attempt will be made to clarify this point after a discussion of the present test results has been made.

During welding the voltage, amperage, and welding speed were recorded and are used in the following equations[8] to compute the cooling rates that exist in the weld at 750 deg. F.

Two-dimensional heat flow:

$$C.R. = 2\pi K \rho C_p \left(\frac{vt}{q}\right)^2 (T' - T_o)^3 \qquad (1)$$

Three-dimensional heat flow:

$$C.R. = 2\pi K \frac{v}{q} (T' - T_o)^2 \qquad (2)$$

where

T_o = Initial plate temperature ($^oF.$)

T' = Temperature at which cooling rate desired ($^oF.$)

K = Thermal conductivity of plate (Btu/ft-hr.-$^oF.$)

v = Velocity of source (in./min.)

ρ = Density of plate (lbs./ft.^{3})

C_p = Specific heat of plate (.155 Btu/lb.-$^oF.$)

t = Plate thickness (inches)

q = Rate of heat flow from source (Btu/hr.)

The value of K varies considerably, but an average value of K = 24 Btu/ft.-hr.-$^oF.$ at 750 deg. F. seems to give fair results.

The possibility that two or three-dimensional heat flow might exist depending on energy input, travel speed, and plate thickness makes

it necessary to calculate the cooling rate for both possible cases. The lower computed cooling rate is the more nearly correct value.(8)

For all of the specimens welded, the calculated cooling rates for both two- and three-dimensional heat flow are listed in Table 7. Also shown in Table 7 is the cracking encountered in each weld. Initially a plot of plate thickness vs. cooling rate was plotted on rectangular coordinate paper (Fig. 23) showing the lower limits of "known cracking" and upper limit of known "no cracking." A curve was drawn as shown on Fig. 23 to represent the approximate critical cooling rate for each plate thickness. It might be noted that additional testing would tend to narrow the band shown on Fig. 23 and, therefore, increase the accuracy of the curve shown on that figure. Equations (1) and (2) were both found to vary linearly on a log-log plot. Equation (1) for each plate thickness tested is plotted in Fig. 36, along with the lower limits of "known cracking" and upper limits of known "no cracking." The curve drawn through the band on the log-log plot is identical to the curve drawn through the band in Fig. 23. The curve in Fig. 23 can be varied merely by adjusting the slope of the straight line on the log-log plot (Fig. 36). This curve shall be referred to hereafter as the critical cooling rate curve and shall be used to define the critical cooling rate at 750 deg. F. for all plate thicknesses referred to in this report. The critical cooling rate for each plate thickness can be determined from Fig. 36. This is the cooling rate at the intersection of the critical cooling rate curve and the curve of Equation (1) for each plate thickness. An example is shown on Fig. 36 for the 3/8-in. plate.

The advantages of using the log-log plot are obvious when one considers the number of tests that would be required to plot the critical

cooling rate curve. Only one series of thick plates and one series of thin plates would be needed, resulting in economy of material and time.

The critical cooling rates, as shown by the critical cooling rate curve on Fig. 36, are plotted assuming that only two-dimensional heat flow away from the weld exists. For thick plates this is obviously not the case; therefore, it is necessary to incorporate the use of Equation (2), which is for three-dimensional heat flow, into the graph shown on Fig. 36. In order to illustrate the three-dimensional heat flow case, it is necessary to refer to Figs. 37 and 38.

Referring first to Fig. 37 and using 1/2-in. plate as an example, the critical cooling rate at 750 deg. F. for 1/2-in. plate is seen to be 112 deg. F./sec. The three-dimensional heat flow case, Equation (2), is represented by the short-dashed line and the two-dimensional heat flow case, Equation (1), by the long-dashed line. Point A represents the transition point from three-dimensional heat flow, for energy input values below point A, to two-dimensional heat flow for energy input values above point A. Actually, there is no sudden transition from the three-dimensional case to the two-dimensional case, therefore, point A represents an approximation of the actual transition.

Returning to the critical cooling rate for the 1/2-in. plate represented by point C on Fig. 37, we find that line B-C represents the minimum energy input/inch that can be used safely while welding 1/2-in. plate to avoid the possibility of microcracking for the electrode-plate combination as used in this investigation. Inspection of the results listed in Table 7 for 1/2-in. plates will show this to be true. Further inspection of Fig. 37 shows that for all <u>safe</u> values of energy input/inch the two-dimensional heat flow condition, Equation (1), will govern; and, therefore, the three-dimensional heat flow case for the 1/2-in. plate need not be considered.

If a thicker plate is considered for which three-dimensional heat flow might govern, the previously stated procedure must be modified slightly. Referring to Fig. 38 and using 1 1/4-in. plate as an example, it is found that point D represents the critical cooling rate, and this value is found to be 62 deg. F./sec. at 750 deg. F. Referring again to point A we see that below point A the three-dimensional heat flow case governs; as a result, point D must be projected down to point C and again line B-C represents the minimum energy input/inch that can be used safely while welding 1 1/4-in. plate and still avoid microcracking for the electrode-plate combination as used in this investigation. Inspection of Table 7 for 1 1/4-in. plate will again show this to be generally true. However, for this case, Table 7 shows that specimen P-1 1/4-4 had an energy input of 31,800 Joules/inch, no cracking, and a calculated cooling rate at 750 deg. F. of 66.5 which is greater than the presumed critical cooling rate of 62 deg. F./sec. Inspection of Fig. 36 shows why this has happened. The critical cooling rate curve on Fig. 36 was drawn at random and could have been drawn within the band for the 1 1/4-in. plate. As the critical cooling rate curve is drawn in Fig. 36, it is believed to be toward the conservative side. This fact is illustrated in the preceding example but still some doubt exists as to the exact critical cooling rate for the 3/4-in. plate due to the width of the band as shown on Fig. 36 for these specimens. Additional testing would be required to narrow the band for the 3/4-in. plate.

The two preceding examples illustrate the use of the log-log plots of energy input vs. cooling rate at 750 deg. F. for both thick and thin plates. A more complete picture is presented by plotting on log-log paper Equation (1) for all plate thicknesses tested, and Equation (2), along with

the critical cooling rate curve from Fig. 36. This has been done on Fig. 39 with the illustrations from Figs. 37 and 38 repeated.

In order to utilize the preceding data, a simple manner of calculating the required energy input per inch or a required electrode travel speed is presented.

Electrode - E-6010 - 3/16-in. diameter

Position - Flat

Recommended

Voltage - 27-29

Current - 170-190

Plate to be welded (assuming a bead-on-plate weld) 3/4-in., ASTM-A7 designation steel.

Using

$$\text{Joules/inch} = \frac{60 \times \text{Volts} \times \text{Amps}}{\text{Speed in in./min.}}$$

$$\text{or} \quad v = \frac{60 \times \text{Volts} \times \text{Amps}}{\text{Energy input}}$$

Examination of Fig. 39 shows that the minimum energy input that can safely be used with 3/4-in. plate is 23,000 Joules/inch.

Therefore

$$v_{Max.} = \frac{60 \times 27 \times 170}{23,000} = 12 \text{ in./min.}$$

$$v_{Max.} = \frac{60 \times 29 \times 190}{23,000} = 14.4 \text{ in./min.}$$

The above calculation assumes that the voltage is arc voltage and current is arc current. A similar calculation can be made for any size electrode and any plate thickness. There is a slight effect on the cooling rate due to electrode size[13][14]; however, the effect is small and can be considered to be of a secondary nature. Hess[13][14] found that increasing

electrode size resulted in a decrease in cooling rate for the same energy input values. The values of critical cooling rates as determined in the investigation reported herein were determined by using a 1/8-in. diameter electrode which would result in maximum cooling rates as far as electrode size is concerned. The results, therefore, tend toward the conservative side. It is also shown in reference[13][14] that the cooling rate is quite independent of electrode type; therefore, it can be assumed that the preceding method used to calculate maximum travel speeds would be equally applicable for any type electrode. This implies also that the type of current used would also have a secondary effect on the cooling rates; however, this has not been verified.

2. Experimental Results

Up to this point no reference has been made to the measured cooling rates nor has the validity of the theoretical cooling rate Equations (1) and (2) for bead-on-plate welds been shown. However, a method has been presented using the cooling rates and plate thicknesses as parameters, that can be used to avoid the possibility of weld metal microcracking for this electrode-plate combination. This would tend to indicate that the errors involved, if any, are more or less constant whether they be in the assumptions regarding efficiency of energy input, thermal properties of the base material, or effect of restraint.

It is believed that the calculated cooling rates are a reasonable approximation of the actual cooling rates that occur. In an attempt to show this, the measured cooling rates shown in Table 7 are plotted on a log-log scale in Fig. 39 and in Fig. 40 on a rectangular coordinate scale. Plotting of the measured cooling rates on the log-log scale (Fig. 39)

tends to distort relationships which otherwise can be seen much clearer on a rectangular coordinate plot. Inspection of either Fig. 39 or Fig. 40 shows that fair agreement exists between theoretical cooling rates and measured cooling rates. However, for the thinner plates, the error seems to increase. This could be the result of a number of factors, but one important factor seems to be that thinner plates tend to lose more heat by radiation and convection than the thicker plates.[13] It can also be seen (See Fig. 40) that a small error in measuring the energy input/inch at low values would produce a larger error than it would for large values of energy input. Even though the number of measured cooling rates is rather limited, the theory as presented previously is still valid. That is, a definite relationship seems to exist for energy input, cooling rate, microcracking, and restraint. This relationship can be used to determine minimum energy input requirements in order to lay sound welds using the electrode-plate combination as used in this investigation. The possibility that similar relationships for other electrodes exist is indicated by results of investigations conducted by others.

Tests conducted at Battelle Memorial Institute by Voldrich[15] show that the following electrodes are susceptible to cold cracking: E-6010, 6011, 6013, 6020, 6030. In connection with the cracking found, Voldrich states that there is a critical cooling rate which, if exceeded, results in a full degree of cold cracking. The investigation, as reported herein, tends to bear out this fact, at least for the E-6010 electrode. It, therefore, seems reasonable that the method of analysis as presented in this report would be applicable to other electrode-plate combinations.

As mentioned previously in this report a discrepancy seems to exist between the results obtained from the fillet weld tests and those

obtained from the bead-on-plate tests. The discrepancy exists in the difference in the critical cooling rates obtained for the different type tests. For the fillet welds a critical cooling rate of 110 deg. F./sec. at 750 deg. F. was found to exist for all welds, while a range of critical cooling rates from 55 deg. F./sec. for 1 1/2-in. plate to 137 deg. F./sec. for 3/8-in. plate was found to exist for the bead-on-plate welds.

Restraint has been shown to be an important factor in determining the critical cooling rate of welds. This has been shown by the bead-on-plate series of welds as reported in this investigation. Residual stresses due to welding are a function of restraint and the degree of restraint is a function of plate thickness as well as joint geometry. The fillet weld specimens as used in Part A have a greater degree of restraint due to geometry than the bead-on-plate specimens as used in the present investigation. It, therefore, seems logical that the fillet weld specimens would also have a greater residual stress due to welding. It follows that the fillet weld specimens should have the lower critical cooling rates.

This has not been the case, however, and an attempt is made to explain this discrepancy by changing the efficiency of the rate of heat flow from source (q) which has been used to calculate the cooling rates as shown in Table 1 of Part A and Table 7 of Part B. It seems logical that the efficiency of the rate of heat flow from the source for fillet welds should be higher than for bead-on-plate welds due to the proximity of the material with respect to the arc during welding. The result is that a greater amount of material will be heated for the fillet weld than for the bead-on-plate weld.

In the initial computations of the cooling rates for both fillet welds and bead-on-plate welds an efficiency of 80 percent for the rate of

heat flow from source was used. The efficiencies are now to be modified so that for fillet welds the energy input is 90 percent efficient, while for bead-on-plate welds 70 percent efficiency will be used. The results obtained when 70 percent efficiency is used for bead-on-plate tests in computing cooling rates are shown in Table 8. Plotted on Fig. 41 are the energy input values vs. cooling rates along with the measured cooling rate values. Table 8 and Fig. 41 are identical to Table 7 and Fig. 39 except for the change in calculated cooling rates due to the change in efficiency. The critical cooling rate curve shown on Fig. 41 was derived in the same manner as the critical cooling rate curves of Figs. 23 and 36.

Inspection of Fig. 41 shows that for all plate thicknesses the critical cooling rate has been increased due to the decrease in efficiency of the rate of heat flow from the source. Also, the overall agreement between measured cooling rates and calculated cooling rates has been improved somewhat.

The change in efficiency of the rate of heat flow from the source from 80 to 90 percent for fillet welds resulted in a general decrease in all cooling rates and thereby reduced the critical cooling rate from 110 deg. F./sec. to approximately 90 deg. F./sec. Listed in Table 9 are the re-calculated cooling rates and the measured cooling rates. In general, increasing the efficiency of energy input for the fillet welds tended to increase the discrepancy between measured cooling rates and calculated cooling rates rather than improve the relationship. This would indicate that the efficiency should probably have been reduced rather than increased in order to give better agreement between measured and calculated cooling rates.

To sum up the relationship between the fillet weld tests and the bean-on-plate tests the following comparison can be made:

The critical cooling rates for the bead-on-plate welds using an efficiency of 80 percent ranged from 55 deg. F./sec. for 1 1/2-in. plate to 137 deg. F./sec. for 3/8-in. plate. Changing the efficiency to 70 percent resulted in a change in the range of critical cooling rates to 63 deg. F./sec. for 1 1/2-in. plate to 183 deg. F./sec. for 3/8-in. plate. The critical cooling rate for all plate thicknesses for the fillet welds using an efficiency of 80 percent was found to be 110 deg. F./sec. Increasing the efficiency to 90 percent resulted in a decrease of the critical cooling rate to approximately 96 deg. F./sec. (See Table 9). The apparent discrepancy still exists, as the critical cooling rate for the bead-on-plate welds for 1 1/2-in. plates is 63 deg. F./sec. (at 70 percent efficiency) while the critical cooling rate found for the fillet weld tests, which included 1 1/2-in. thick plates, is approximately 96 deg. F./sec. (at 90 percent efficiency).

The preceding results are contrary to what was anticipated as the fillet weld test was assumed to have a greater degree of restraint (due to geometry) and, therefore, should have had the lower critical cooling rate. It is fairly obvious that the discrepancy is not entirely due to the choice of efficiency of energy input used in calculating the cooling rates. The exact reasons for the discrepancy are not readily determined, and a considerable amount of additional testing would be required to resolve the problem. More accurate methods are needed to measure cooling rates encountered in order to determine the exact efficiency of the rate of heat flow from the source for various types of

welds. Measurement of residual strains would also help to relate different types of test specimens to one another. An attempt to measure residual strains was undertaken during this investigation; however, the results were found to be very inconsistent and, therefore, considered to be of little value and were discarded.

Even though a relationship between the bead-on-plate tests and the fillet weld tests has not been established, the results of the individual investigations are still consistent within themselves. It, therefore, appears that each type of test is still valid and can be used successfully to predict results of welds under similar conditions within a welded structure. However, at the present time no attempt should be made to relate results of one weldability test to another unless geometrical configurations and restraint conditions are very similar. This implies that weldability tests should duplicate actual service requirements as closely as possible.

Service conditions rarely, if ever, would require depositing a bead-on-plate type of weld, but numerous butt welds might be required. It would, therefore, be desirable to relate the theory as reported in this investigation to butt welds and cracking encountered in butt welds. Hess, etal,[13][14] developed a series of equations that could be used to predict cooling rates encountered in the heat-affected zone for butt and fillet welds. The equations are approximately linear on a log-log scale, and fair agreement can be shown to exist between the theoretical equations as used in this report and the equations developed by Hess. Hess' equations for various plate thicknesses do not plot parallel to one another on a log-log plot; therefore, the critical cooling rate curve as shown on

Fig. 36 cannot be utilized, thus complicating the problem somewhat. The experimental results of references (13) and (14) could very well be applied to the theory as reported herein indicating that the theory presented in this report could easily be applied to butt welds.

Severe cracking is occasionally encountered in butt welds. The possibility exists that the cracking encountered could be related to cooling rates and restraint; therefore, a method of interpreting results similar to that used in this report would prove to be a valuable tool. Not only butt welds but other types of test specimens could very well be analyzed in a similar manner; however, in order to establish relationships between tests, a considerable amount of additional testing would be required.

The possibility of weld cracking should not be the only factor considered in weldability tests. Tests that determine physical properties, such as ductility, impact resistance, hardness, and fatigue strength must also be included in order to assure that welded structures will perform satisfactorily under service conditions.

XIV. CONCLUSIONS

A sufficient number of specimens of each plate thickness, except 1 1/2-in. thick plate, were tested so that a transition was found from microcracking in the weld metal to "no microcracking" in the weld metal. These results permitted the band shown on Fig. 23 to be plotted. Additional testing would undoubtedly decrease the width of the band and thereby establish a more exact critical cooling rate for each plate thickness. Only mechanical polishing methods have been used; it, therefore, remains possible that electro-polishing methods might change the critical cooling rate somewhat by disclosing additional cracking. However, the following general conclusions seem justified from the results of the investigation conducted using the E-6010 electrode and A-7 steel combination.

1. It is not necessary to have a highly restrained condition to induce microcracking in the weld metal of an E-6010 electrode weld deposited on ASTM designation A-7 steel.
2. The critical cooling rate was found to decrease with increasing plate thickness. This is believed to be a function of increased restraint due to the increased plate thickness; however, inspection of Figs. 23 and 40 shows that as plate thickness increases, the critical cooling rate approaches a minimum value very rapidly. For all practical purposes, a minimum critical cooling rate of 50 deg. F./sec. at 750 deg. F. for plate thicknesses greater than 1 1/2-in. could be used.
3. Plotting the theoretical cooling rate equations on a log-log scale and superimposing a critical cooling rate curve (from Fig. 23) presents a rapid and simple means of determining

minimum energy input requirements that are necessary to avoid the possibility of microcracking in the weld metal for the electrode-plate combination as used in this investigation.

4. It is believed that the method of calculating cooling rates and presenting the results in graphical form such as Fig. 39 can be expanded to most types of weld cracking where restraint and cooling rate are important variables.

5. It is difficult to establish relationships between different types of test specimen configurations; however, the results of individual tests should be directly applicable to similar type geometrical conditions encountered under service conditions.

BIBLIOGRAPHY

1. Cottrell, C. L. M., "Controlled Thermal Severity Cracking Test Simulates Practical Welded Joints," Welding Journal, June, 1953.

2. Berry, J. T. and Allen, R. C., "A Study of Cracking in Low Alloy Steel Welded Joints," Welding Journal, March, 1960.

3. Flanigan, A. E. and Kaufman, M., "Microcracks and the Low Temperature Cooling Rate Embrittlement of Welds," Welding Journal, December, 1951.

4. Hoyt, S. L., Sim, C. E., and Banta, H. M., "Metallurgical Factors of Underbead Cracking," Transactions A.I.M.E., Vol. 162, 1945.

5. Christensen, N., "Metallurgical Aspects of Welding Mild Steel," Welding Journal, Vol. 28, part 2, 1949.

6. Winterton, R. and Nolan, M. J., "Factors Affecting Severity of Cruciform Test for Hardened Zone Cracking," Welding Journal, February, 1960.

7. Poteat, L. E. and Warner, W. L., "The Cruciform Test for Plate Cracking Susceptibility," Welding Journal, February, 1960.

8. Adams, C. M., "Cooling Rates and Peak Temperatures in Fusion Welding," Welding Journal, May, 1958.

9. Stout, R. D. and Doty, W. D., "Weldability of Steels," Welding Research Council, New York City, 1953, pp. 90-95.

10. Payson, P. and Grange, R. A., "The Temperature Range of Martensite Formation in Steel," Metals Handbook, 1948, pp. 611-612.

11. Flanigan, A. E. and Micheu, T., "Relation of Preheating to Embrittlement and Microcracking in Mild Steel Welds," Welding Journal, February, 1953.

12. Flanigan, A. E. and Saperstein, Z. P., "Isothermal Studies on the Weld Metal Microcracking of Arc Welds in Mild Steel," Welding Journal, November, 1956.

13. Hess, W. F., etal, "The Measurement of Cooling Rates Associated With Arc Welding and Their Application to the Selection of Optimum Welding Conditions," Welding Journal, Part II 22, 1943.

14. Hess, W. F., etal, "Determination of Cooling Rates of Butt and Fillet Welds as a Result of Arc Welding with Various Types of Electrodes on Plain Carbon Steel," Welding Journal 23, 1944, pp. 376s-391s.

15. Voldrich, C. B., "Cold Cracking in the Heat-affected Zone," Welding Journal, Part I 26, 1947, pp. 153s-169s.

TABLE 1

SUMMARY OF SPECIMENS TESTED IN PART A, ENERGY INPUTS, COOLING RATES AT 750°F AND DEGREE OF CRACKING

Specimen	Plate Thickness Top	Plate Thickness Bottom	Electrode Size	Weld No.	Travel Speed (in./min.)	Energy Input (Joules/inch)	Cooling Rates at 750°F. (°F./sec.) Calculated 2-Dimensional	Calculated 3-Dimensional	Measured	Cracks Fig. 18 Type	Cracks Fig. 5 Type
D-12-1	1/2"	1/2"	1/8"	1	9.23	21,100	Quenched		-	1/inch	
C-12-1	1/2	1/2	1/8	2	13.35	14,240	228.0	225.0	-	16/inch	
C-12-1	1/2	1/2	1/8	1	8.74	16,200	(*) 171.0	197.0	249	4/inch	
B-34-1	3/4	3/4	1/8	1	10.44	18,750	296.0	171.0	175	3/inch	
C-34-1	3/4	3/4	1/8	1	10.00	18,970	289.0	168.0	200	--	
B-1-2	1	1	1/8	1	10.00	18,950	514.0	168.0	225	2/inch	
C-34-1	3/4	3/4	1/8	2	9.60	19,900	263.0	160.0	194	4/inch	
B-1-2	1	1	1/8	2	9.24	20,000	462.0	160.0	-	--	90%
B-34-1	3/4	3/4	1/8	2	9.24	20,700	242.0	154.0	-	--	60%
B-12-1	1/2	1/2	1/8	1	9.60	19,800	(*) 117.0	161.0	-	None	
B-1-1	1	1	1/8	1	6.77	28,500	229.0	112.5	-	None	
B-1-1	1	1	1/8	2	6.67	28,500	237.0	112.0	-	2 Very Minute	20%
B-15-1	1-1/2	1-1/2	3/16	2	9.23	29,650	475.0	107.8	-	None	
B-15-1	1-1/2	1-1/2	3/16	1	8.58	31,900	410.0	100.0	-	None	
C-15-1	1-1/2	1-1/2	3/16	2	8.00	33,500	371.0	95.4	-	--	
B-12-1	1/2	1/2	1/8	2	8.58	22,000	(*) 94.4	144.0	-	None	
C-1-1	1	1	3/16	2	7.75	36,300	140.0	88.0	88	None	
C-15-1	1-1/2	1-1/2	3/16	1	6.58	40,800	251.0	78.6	-	--	
D-12-1	1/2	1/2	1/8	2	7.06	27,600	(*) 75.4	134.0	-	None	
C-1-1	1	1	3/16	1	5.34	51,500	69.8	62.2	71	None	

\- Indicates insufficient data.
(*) 2-Dimensional heat flow governed.
-- Indicates - not examined.

Note - Specimens listed in descending order of governing cooling rates.

TABLE 2

TRAVEL SPEEDS REQUIRED TO DEPOSIT GIVEN FILLET SIZE

Electrode Size	Recommended Volts	Recommended Amps	Selected Fillet Size	Energy Input Required (Joules/inch)	Travel Speed Required (In/Min.) Minimum	Travel Speed Required (In/Min.) Maximum
1/8"	25-27	110-130	1/8"	10,500	15.7	20.0
1/8	25-27	110-130	3/16	20,000	8.25	10.50
5/32	27-29	140-160	1/4	33,500	6.75	8.30
3/16	27-29	170-190	5/16	47,500	5.86	7.04
7/32	28-30	220-250	3/8	60,000	6.16	7.50
1/4	28-32	240-300	1/2	87,200	4.62	6.60
1/4	28-32	240-300	5/8	114,000	3.54	5.06

Table 2 is for use with A.O. Smith E-6010 electrodes used in the flat position only.

TABLE 3

AWS SPECIFICATION REQUIREMENTS FOR FILLET SIZES
& CORRESPONDING CALCULATED COOLING RATES

Plate Thickness Top	Plate Thickness Bottom	Minimum Fillet Size	Minimum Travel Speed	Calculated Cooling Rates @750°F 3-Dimensional	Calculated Cooling Rates @750°F 2-Dimensional
(*) 1/4"	1/4"	3/16"	8.25 in/min.	160°F./sec.	* 28.9°F./sec.
1/2	1/2	3/16	8.25	160	* 115
3/4	3/4	1/4	6.75	95	* 92
1-1/2	1-1/2	5/16	5.86	* 67.3	185
2-1/4	2-1/4	3/8	6.16	* 53.3	261
6	6	1/2	4.62	* 36.8	878

(*) Not listed in specifications.
Cooling rates were computed for minimum travel speeds utilizing minimum recommended voltage and amperage for computing rate of heat flow.

* Governing calculated cooling rates.

TABLE 4

AWS SPECIFICATIONS FOR FILLET SIZES AND THOSE
RECOMMENDED IN THIS REPORT

Specifications		Recommended	
Plate Thickness	Minimum Fillet Size	Plate Thickness	Minimum Fillet Size
To 1/2"	3/16"	To 1/4"	3/16"
1/2 - 3/4	1/4	Over 1/4	1/4
3/4 - 1-1/2	5/16		
1-1/2 - 2-1/4	3/8		
2-1/4 - 6	1/2		
Over 6	5/8		

TABLE 5

COOLING RATES AT 572°F (300°C) AND DEGREE OF CRACKING

Specimen	Weld No.	Calculated Cooling Rate at 572°F. (°F./sec.) 2-Dimensional	3-Dimensional	Governing	Measured Cooling Rate at 572°F. °F/sec.	Cracks Fig. 18 Type	Fig. 5 Type
D-12-1	1		Quenched		-	1/inch	
B-34-1	1	128.2	100.6	100.6	152.0	3/inch	
B-1-2	1	223.0	99.6	99.6	145.5	3/inch	
C-34-1	1	125.0	99.5	99.5	137.0	-	
C-12-1	2	99.2	133.0	99.2	116.0	16/inch	
C-34-1	2	113.5	94.6	94.6	121.5	4/inch	
B-1-2	2	200.5	94.4	94.4	138.0	-	90% of weld
B-34-1	2	105.0	91.1	91.1	138.0	-	60% of weld
C-12-1	1	76.3	116.5	76.5	131.0	4/inch	
B-1-1	1	99.6	66.5	66.5	-	None	
B-1-1	2	98.7	66.1	66.1	75.0	(2/inch - very minute)	20% of weld
B-15-1	2	205.0	63.6	63.6	-	None	
B-15-1	1	177.5	59.2	59.2	-	None	
C-15-1	2	161.0	56.4	56.4	60.5	-	
C-1-1	2	61.0	52.0	52.0	69.7	None	
B-12-1	1	50.9	95.0	50.9	-	None	
C-15-1	1	109.2	46.4	46.4	-	-	
B-12-1	2	40.8	85.0	40.8	72.8	None	
D-12-1	2	34.9	82.5	34.9	-	None	
C-1-1	1	30.3	36.6	30.3	47.7	None	

TABLE 6

PHYSICAL PROPERTIES OF MATERIAL TESTED

Chemical Analysis - Base Material							
Specimen	C	Mn	Si	P	S	Ni	Cu
1 1/4" plate	.17	.90	.14	.012	.032	.03	.07
3/4" plate	.18	.76	.01	.012	.030	.02	.01
3/8" plate	.17	.67	.02	.014	.038	.03	.04
Electrode (*)	.08	.47	.21	.022	.026	-	-

Tensile Tests			
Specimen	Lower Yield Stress	Ultimate Stress	Elongation
1 1/4" plate	30.2 ksi	57.7 ksi	35%
1 1/4" plate	34.1	60.2	31.5
3/4" plate	38.8	59.3	35
3/4" plate	33.7	59.8	-
Electrode (*)	59.2	71.15	29.9

(*) Manufacturer's listed value.

TABLE 7

SUMMARY OF SPECIMENS TESTED IN PART B, ENERGY INPUTS, COOLING RATES AND DEGREE OF CRACKING
(Efficiency of rate of heat flow from source = 80%)

Specimen	Plate Thickness (inches)	Energy Input (Joules/inch)	Cooling Rates at 750° F. (°F./sec.) Calculated 2D***	Calculated 3D****	Measured	Cracks
P-3/8-3	3/8	7,830	*187.0	270.0	-	3/inch
P-3/8-5	"	8,540	*158.0	248.0	203.0	3/inch
P-3/8-4	"	9,640	*124.0	220.0	158.0	none
P-3/8-7	"	10,300	*110.0	207.0	-	none
P-3/8-6	"	11,300	* 90.5	188.0	-	none
**P-3/8-2	"	16,600	* 41.0	126.0	-	none
P-3/8-8	"	17,800	* 36.8	120.0	68.3	none
**P-3/8-1	"	17,500	* 36.7	119.4	-	none
P-1/2-4	1/2	11,340	*161.0	187.0	-	8/inch
P-1/2-5	"	12,680	*128.4	167.0	-	12/inch
P-1/2-3	"	13,680	*110.0	155.0	178.0	none
P-1/2-2	"	14,300	*100.5	148.0	132.0	none
P-1/2-6	"	21,200	* 45.8	100.0	-	none
P-1/2-1	"	25,800	* 30.8	82.0	-	none
P-3/4-1	3/4	18,000	142.0	*118.0	157.0	13/inch
P-3/4-2	"	20,200	112.0	*105.0	141.0	9/inch
P-3/4-6	"	28,300	* 57.5	74.5	88.5	none
P-3/4-3	"	33,200	* 42.0	64.0	-	none
P-3/4-5	"	34,800	* 38.3	61.0	-	none
P-3/4-4	"	43,700	* 24.3	48.6	-	none
P-1 1/4-1	1 1/4	21,300	286.0	* 99.5	-	5/inch
P-1 1/4-2	"	26,200	188.0	* 81.0	89.4	1/inch
P-1 1/4-3	"	28,900	155.0	* 73.5	-	2/inch
P-1 1/4-4	"	31,800	127.0	* 66.5	69.8	none
P-1 1/4-5	"	37,000	94.0	* 57.3	-	none
P-1 1/4-6	"	42,200	73.0	* 50.5	53.3	none
P-1 1/2-5	1 1/2	16,850	650.0	*125.5	-	6/inch
P-1 1/2-4	"	18,580	535.0	*113.8	119.5	4/inch
P-1 1/2-3	"	22,000	383.0	* 96.2	95.2	20/inch
P-1 1/2-6	"	22,900	330.0	* 89.5	-	4/inch
P-1 1/2-2	"	31,400	186.8	* 67.3	-	1/inch
P-1 1/2-1	"	36,100	141.6	* 58.6	-	11/inch

* Lowest values - therefore, governing cooling rates.

** Initial plate temperature measured to be 77°F.

*** Two dimensional heat flow.

**** Three dimensional heat flow.

TABLE 8

SUMMARY OF SPECIMENS TESTED IN PART B, ENERGY INPUTS, COOLING RATES AND DEGREE OF CRACKING
(Efficiency of rate of heat flow from source = 70%)

Specimen	Plate Thickness (inches)	Energy Input (Joules/inch)	Cooling Rates at 750°F. (°F./sec.) Calculated 2D***	Calculated 3D****	Measured	Cracks
P-3/8-3	3/8	7,830	*245.0	308.0	-	3/inch
P-3/8-5	"	8,540	*207.0	283.0	203.0	3/inch
P-3/8-4	"	9,640	*162.5	251.0	158.0	none
P-3/8-7	"	10,300	*144.0	236.0	-	none
P-3/8-6	"	11,300	*118.5	224.4	-	none
**P-3/8-2	"	16,600	* 53.7	143.8	-	none
P-3/8-8	"	17,800	* 48.2	137.0	68.3	none
**P-3/8-1	"	17,500	* 48.1	136.0	-	none
P-1/2-4	1/2	11,340	*211.0	213.0	-	8/inch
P-1/2-5	"	12,680	*168.0	190.5	-	12/inch
P-1/2-3	"	13,680	*144.0	177.0	178.0	none
P-1/2-2	"	14,300	*131.6	168.8	132.0	none
P-1/2-6	"	21,200	* 60.0	114.0	-	none
P-1/2-1	"	25,800	* 40.4	93.5	-	none
P-3/4-1	3/4	18,000	186.0	*134.6	157.0	13/inch
P-3/4-2	"	20,200	146.8	*119.8	141.0	9/inch
P-3/4-6	"	28,300	* 75.4	85.0	88.5	none
P-3/4-3	"	33,200	* 55.0	73.0	-	none
P-3/4-5	"	34,800	* 50.2	69.6	-	none
P-3/4-4	"	43,700	* 31.8	56.6	-	none
P-1 1/4-1	1 1/4	21,300	375.0	*113.5	-	5/inch
P-1 1/4-2	"	26,200	246.0	* 92.4	89.4	1/inch
P-1 1/4-3	"	28,900	203.0	* 83.8	-	2/inch
P-1 1/4-4	"	31,800	166.5	* 75.8	69.8	none
P-1 1/4-5	"	37,000	123.0	* 65.4	-	none
P-1 1/4-6	"	42,200	95.6	* 57.5	53.3	none
P-1 1/2-5	1 1/2	16,850	852.0	*143.0	-	6/inch
P-1 1/2-4	"	18,580	701.0	*129.8	119.5	4/inch
P-1 1/2-3	"	22,000	502.0	*109.8	95.2	20/inch
P-1 1/2-6	"	22,900	432.0	* 98.1	-	4/inch
P-1 1/2-2	"	31,400	245.0	* 73.8	-	1/inch
P-1 1/2-1	"	36,100	185.5	* 64.3	-	11/inch

* Lowest values - therefore, governing cooling rates.

** Initial Plate Temperature Measured to be 77°F.

*** Two dimensional heat flow.

**** Three dimensional heat flow.

TABLE 9

SUMMARY OF SPECIMENS TESTED IN PART A, ENERGY INPUTS, COOLING RATES AND DEGREE OF CRACKING
(Efficiency of rate of heat flow from source changed from 80% in Part A to 90% in this table)

Specimen	Weld No.	Energy Input (Joules/inch)	Cooling Rates at 750°F. (°F./sec.) Calculated 2D**	3D***	Measured	Cracks
D-12-1	1	21,100	Quenched		-	1/inch
C-12-1	2	14,240	*180.0	200.0	-	16/inch
B-34-1	1	18,750	234.0	*152.0	175.0	3/inch
C-34-1	1	18,970	229.0	*149.5	200.0	-
B-1-2	1	18,950	406.0	*149.5	225.0	2/inch
C-34-1	2	19,900	208.0	*142.0	194.0	4/inch
B-1-2	2	20,000	365.0	*142.0	-	-
B-34-1	2	20,700	191.5	*137.0	-	-
C-12-1	1	16,200	*135.0	175.0	249.0	4/inch
B-1-1	1	28,500	181.0	*100.0	-	none
B-1-1	2	28,500	187.5	* 99.7	-	2/inch
B-15-1	2	29,650	376.0	* 95.8	-	none
B-12-1	1	19,800	* 92.5	143.0	-	none
B-15-1	1	31,900	324.0	* 88.9	-	none
C-15-1	2	33,500	293.0	* 84.7	-	-
C-1-1	2	36,300	110.5	* 78.2	88.0	none
B-12-1	2	22,000	* 74.6	128.0	-	none
C-15-1	1	40,800	198.5	* 69.8	-	-
D-12-1	2	27,600	* 59.6	119.0	-	none
C-1-1	1	51,500	* 55.2	55.3	71.0	none

* Governing calculated cooling rate.

** Two dimensional heat flow.

*** Three dimensional heat flow.

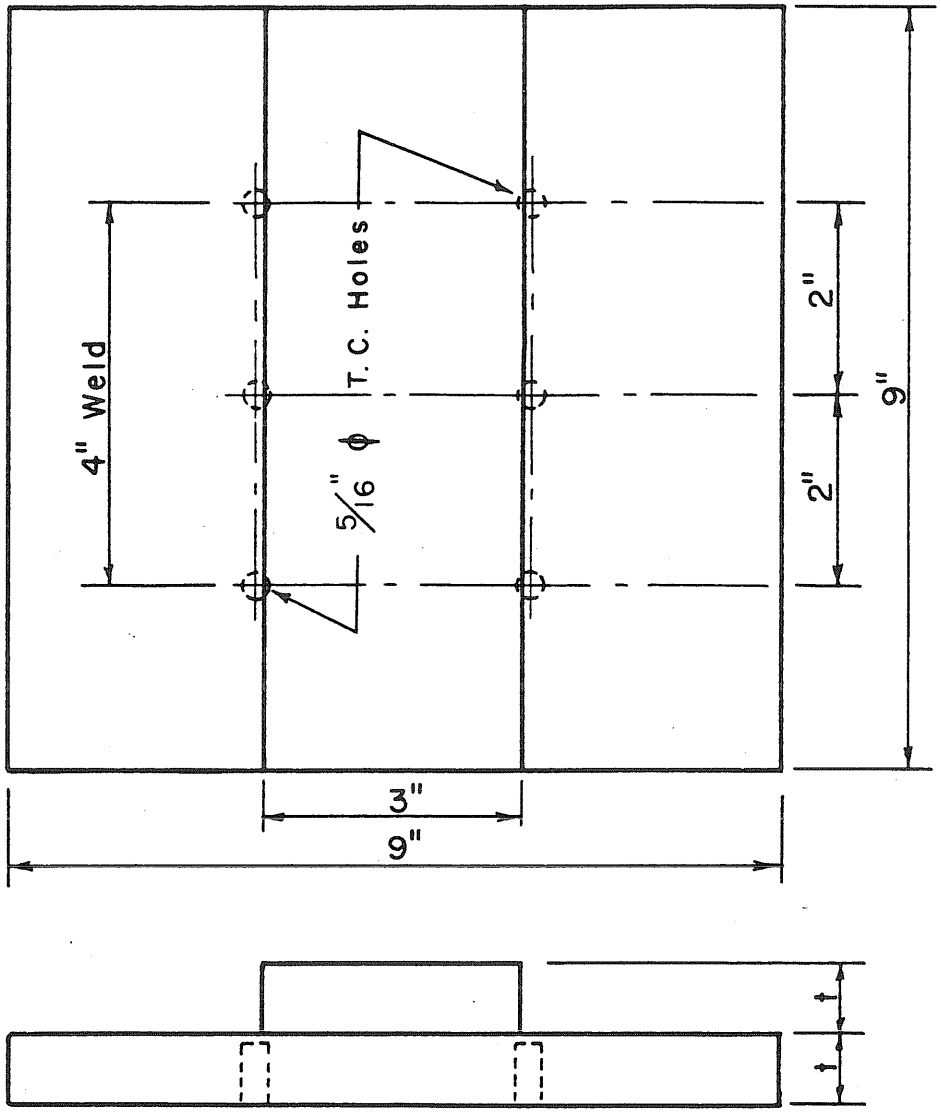

DETAILS OF FILLET WELD SPECIMEN

Fig. 1

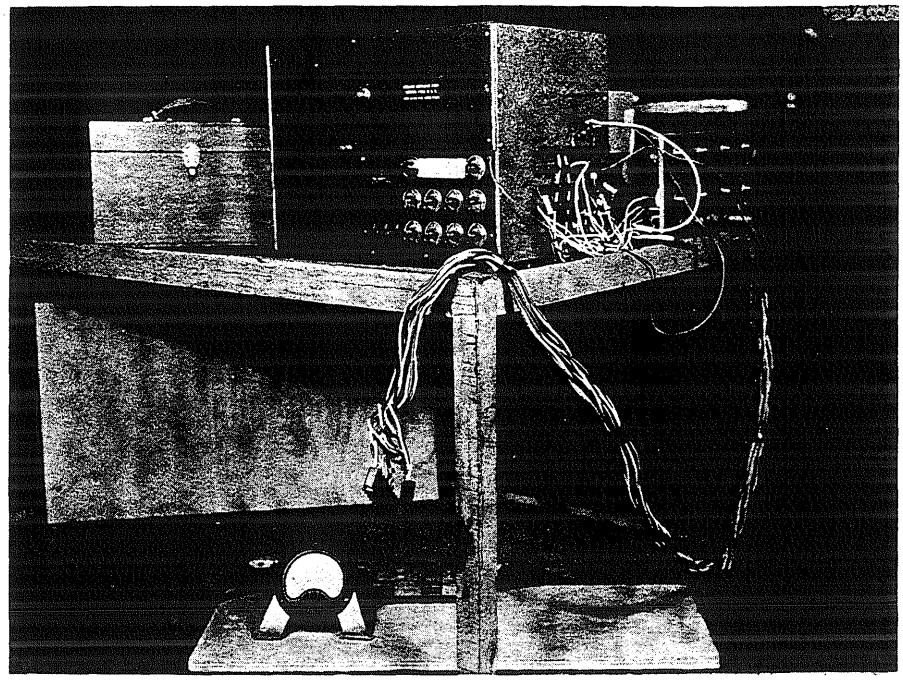

Fig. 2 General View of Instrumentation

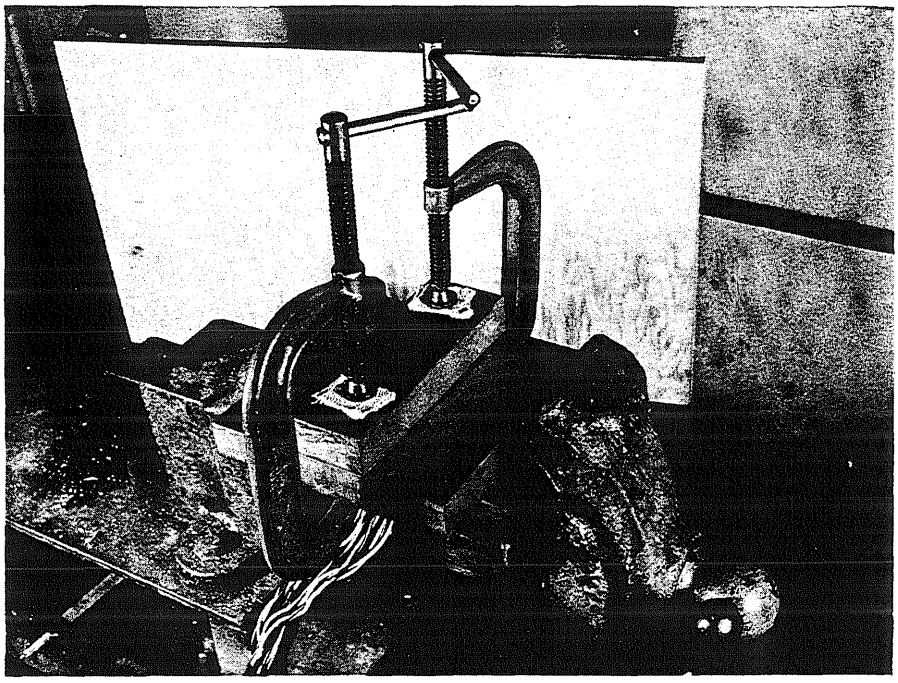

Fig. 3 Specimen Assembled for Welding

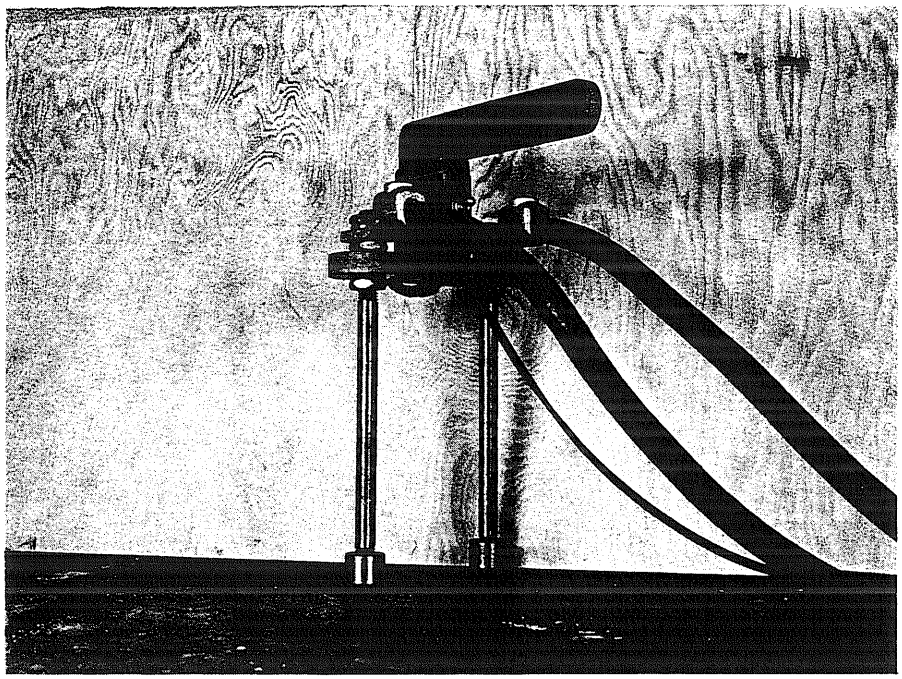

Fig. 4 Portable Magnaflux Prods

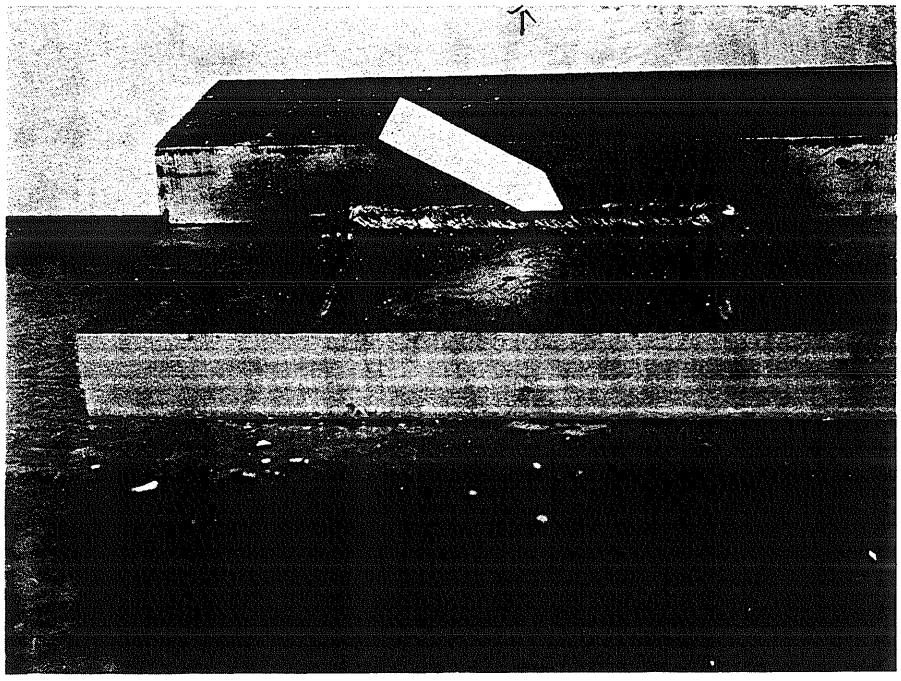

Fig. 5 Iron Powder Showing Crack in Magnetized Specimen

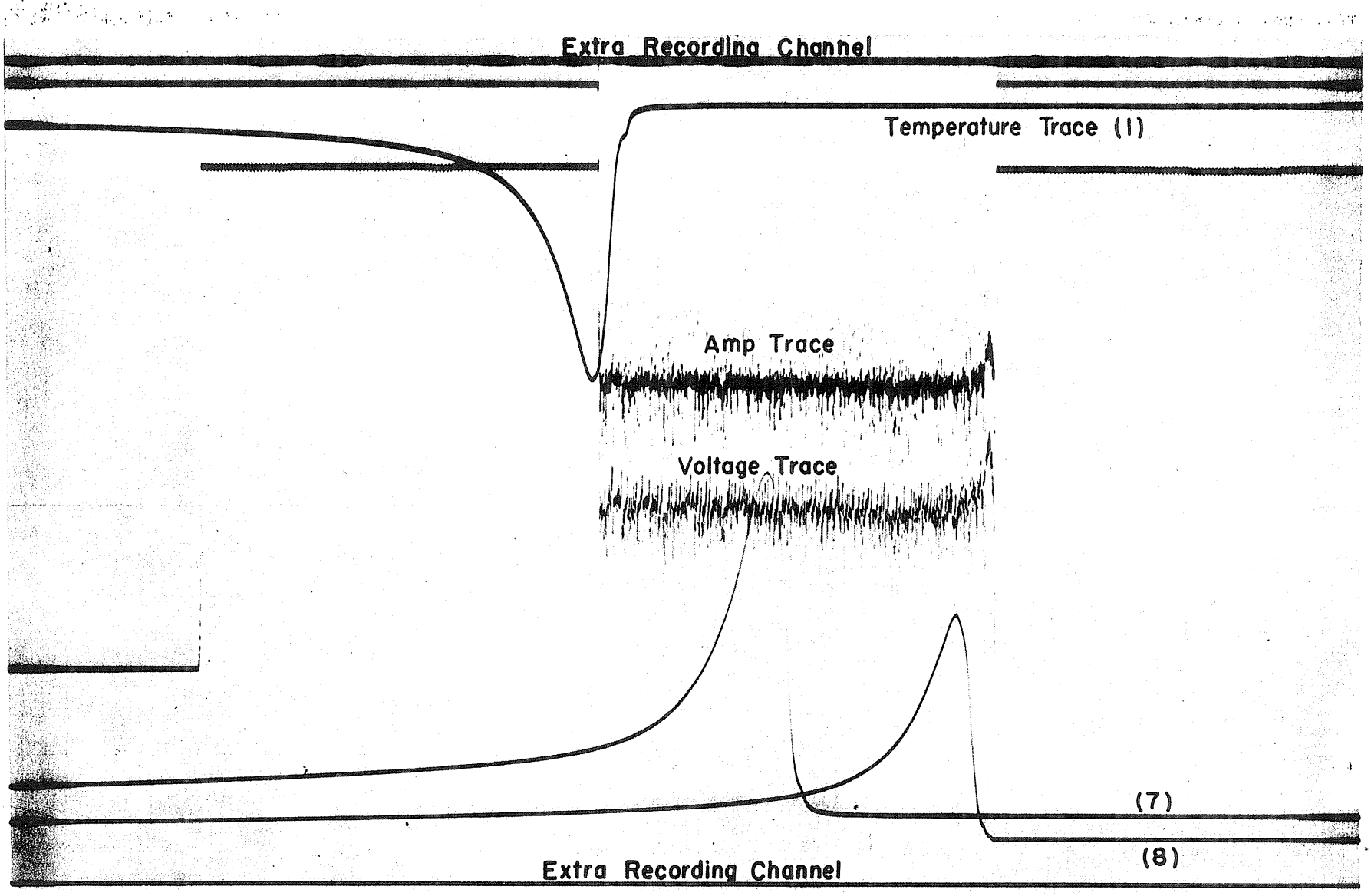

FIG. 6 TYPICAL OSCILLOGRAM FOR DETERMINATION OF COOLING CURVES & ENERGY

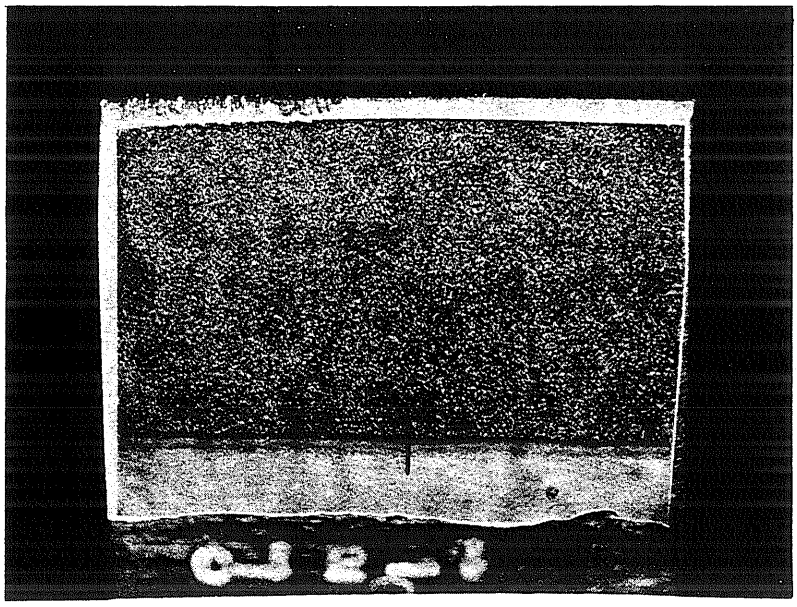

Fig. 7 Macrograph Showing Typical Polished & Etched Specimen (Location of Hardness Survey Shown)

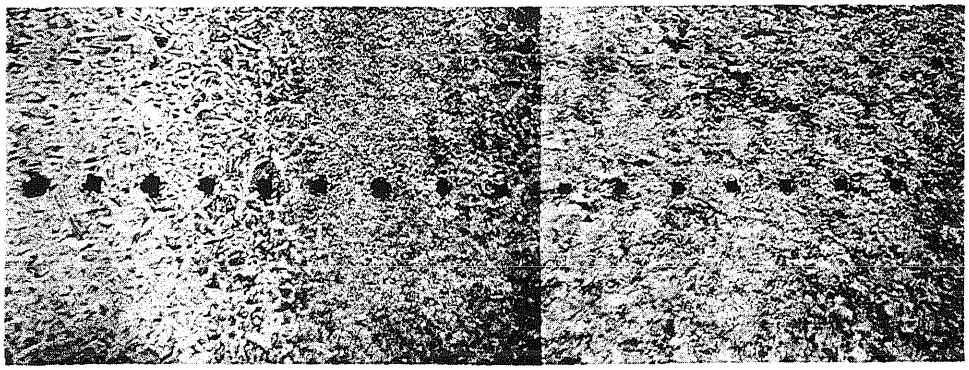

Fig. 8 Location of Hardness Survey

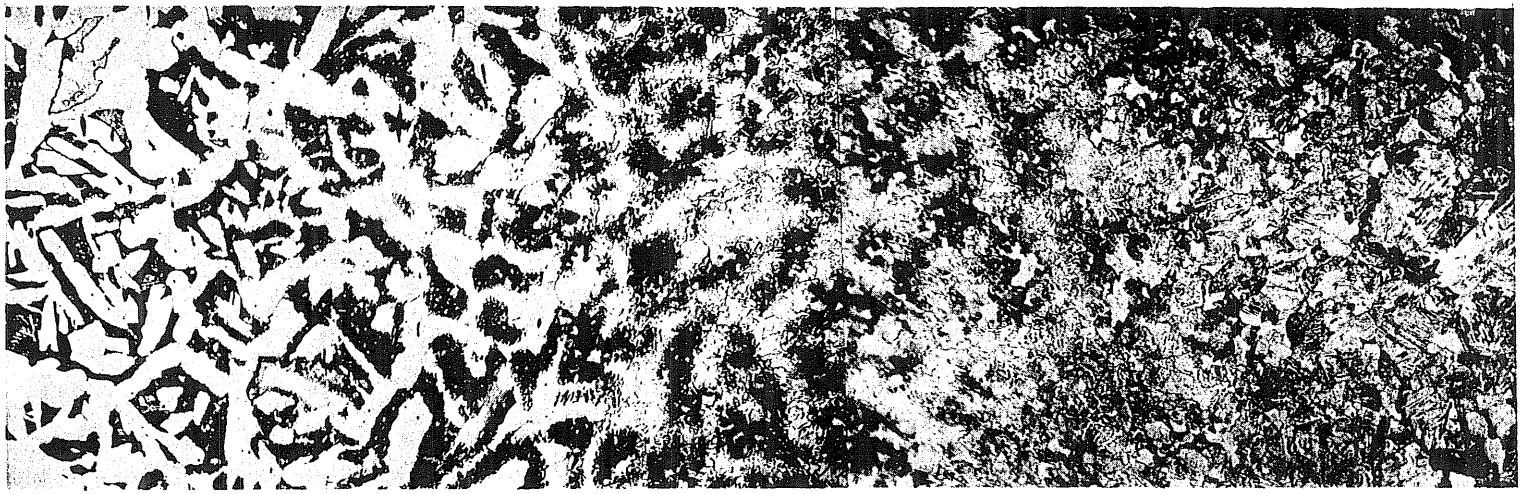

Base Metal

Heat Affected Zone

Fusion Line

Weld Metal

(This Specimen Had Slight Cracking)

Fig. 9 Specimen D-12-1 Weld No. 1, Quenched After Welding

(x 200)

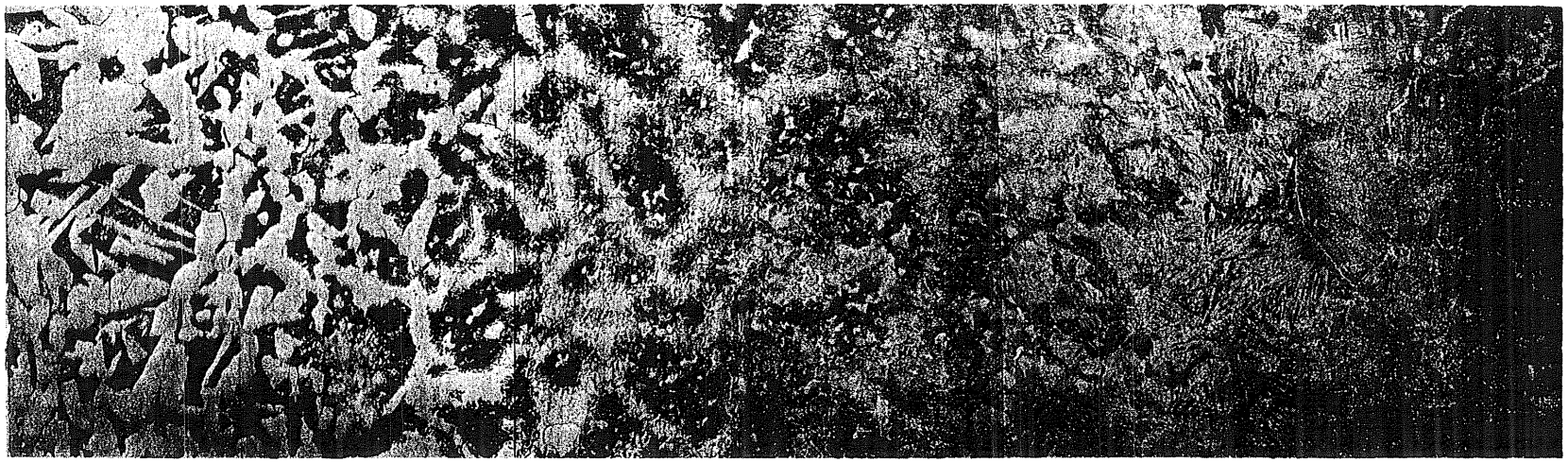

(This Specimen Had Severe Cracking)

Fig. 10 Specimen C-12-1 Weld No. 2, Cooling Rate at 750°F = 225°F/sec. (x 200)

(This Specimen Had Slight Cracking)

Fig. 11 Specimen B-1-2 Weld No. 1, Cooling Rate at 750°F = 168°F/sec. (x 200)

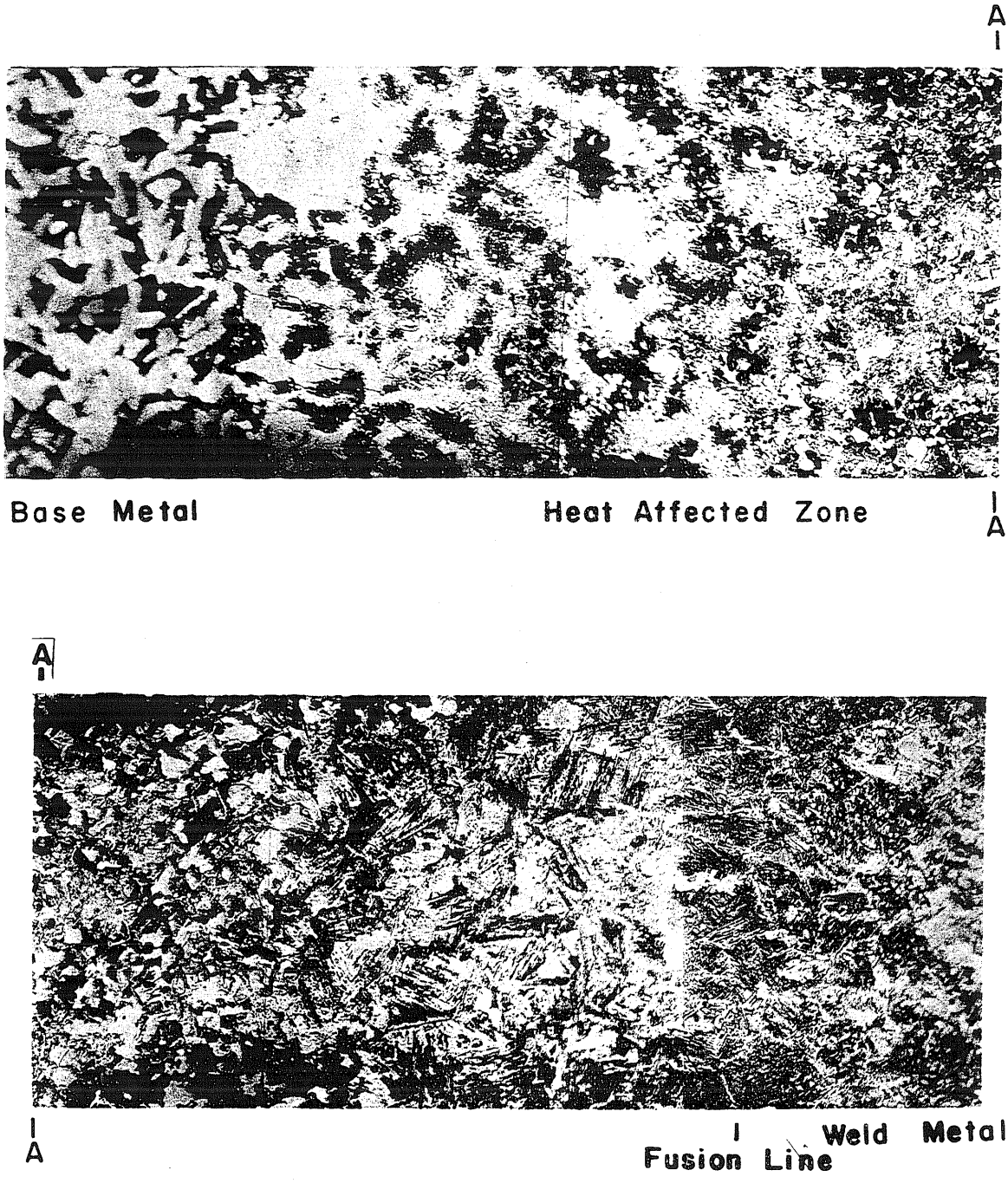

(This Specimen Had No Cracking)

Fig. 12 Specimen B-12-1 Weld No. 2, Cooling Rate at 750°F = 94.4 °F/sec. (x 200)

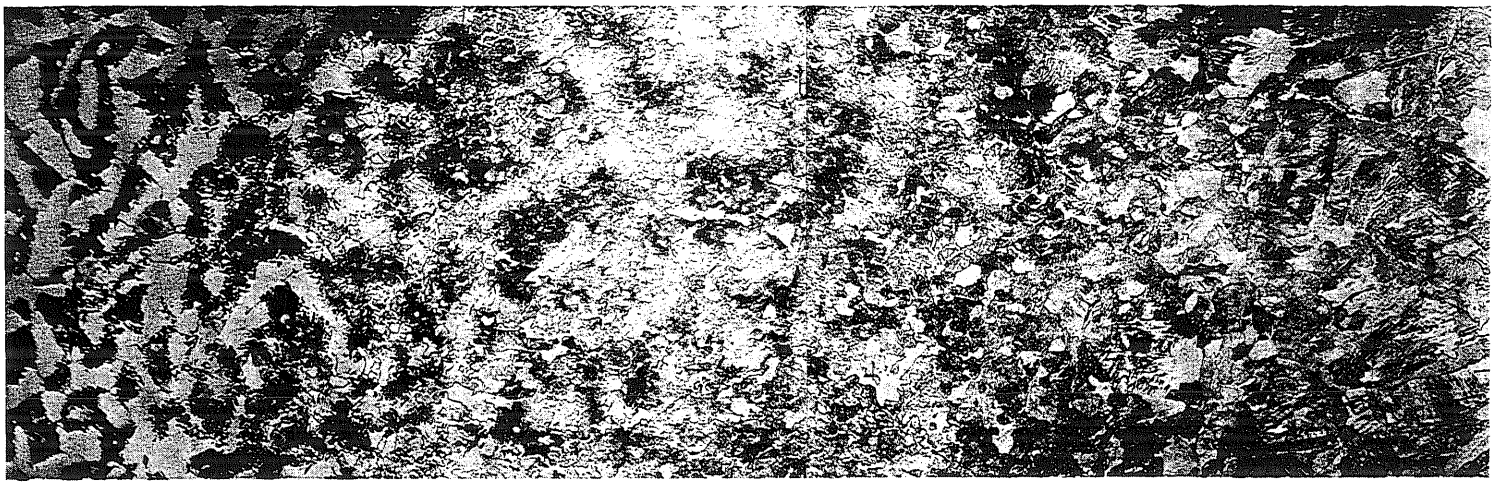

Base Metal to Fusion Line

Weld Metal

(This Specimen Had No Cracking)

Fig. 13 Specimen D-12-1 Weld No. 2, Cooling Rate at 750°F = 75.4°F/sec.

Ambient Temperature = 20°F

(x 200)

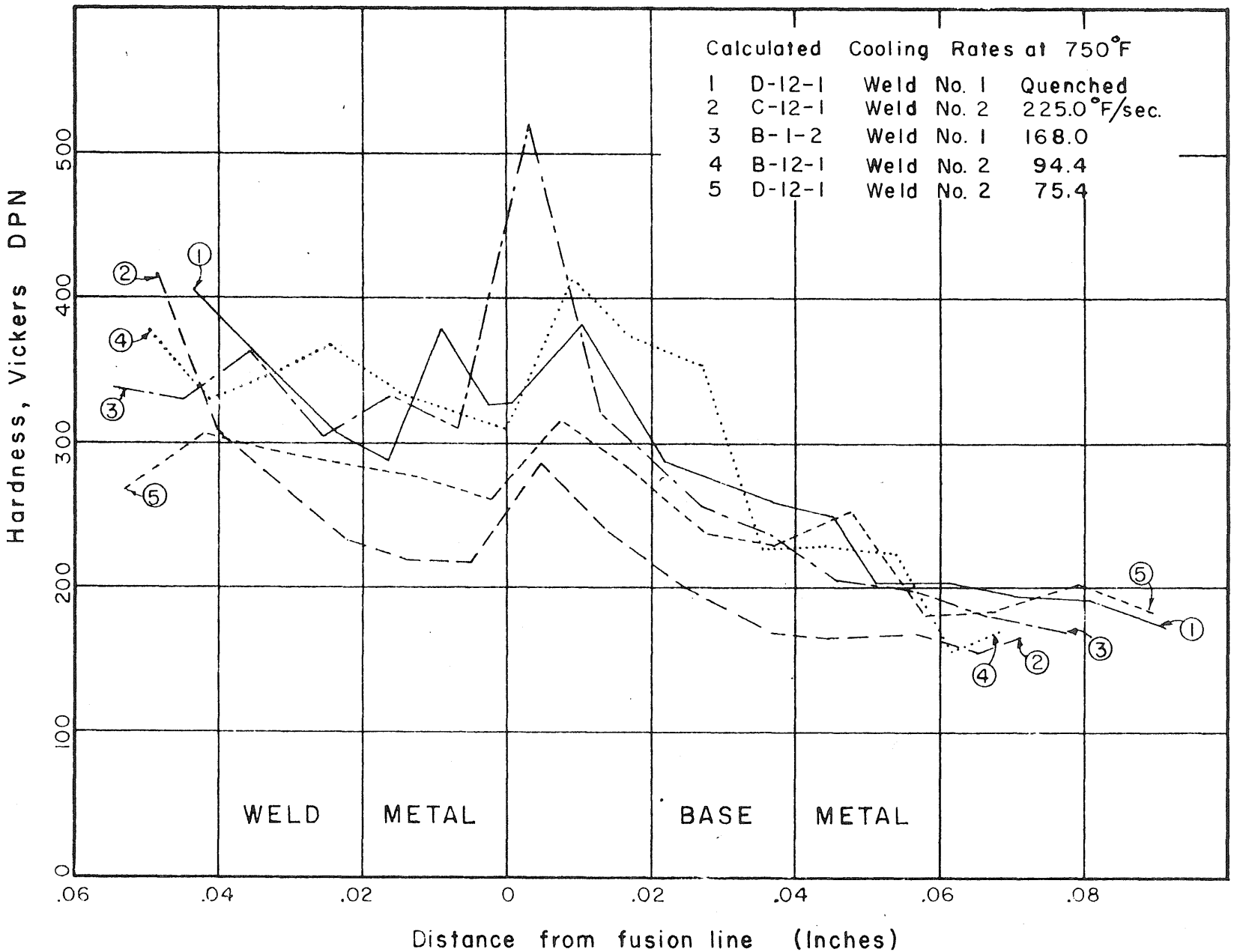

Fig. 14 Hardness Surveys of Specimens Shown in Fig. 9 Through 13

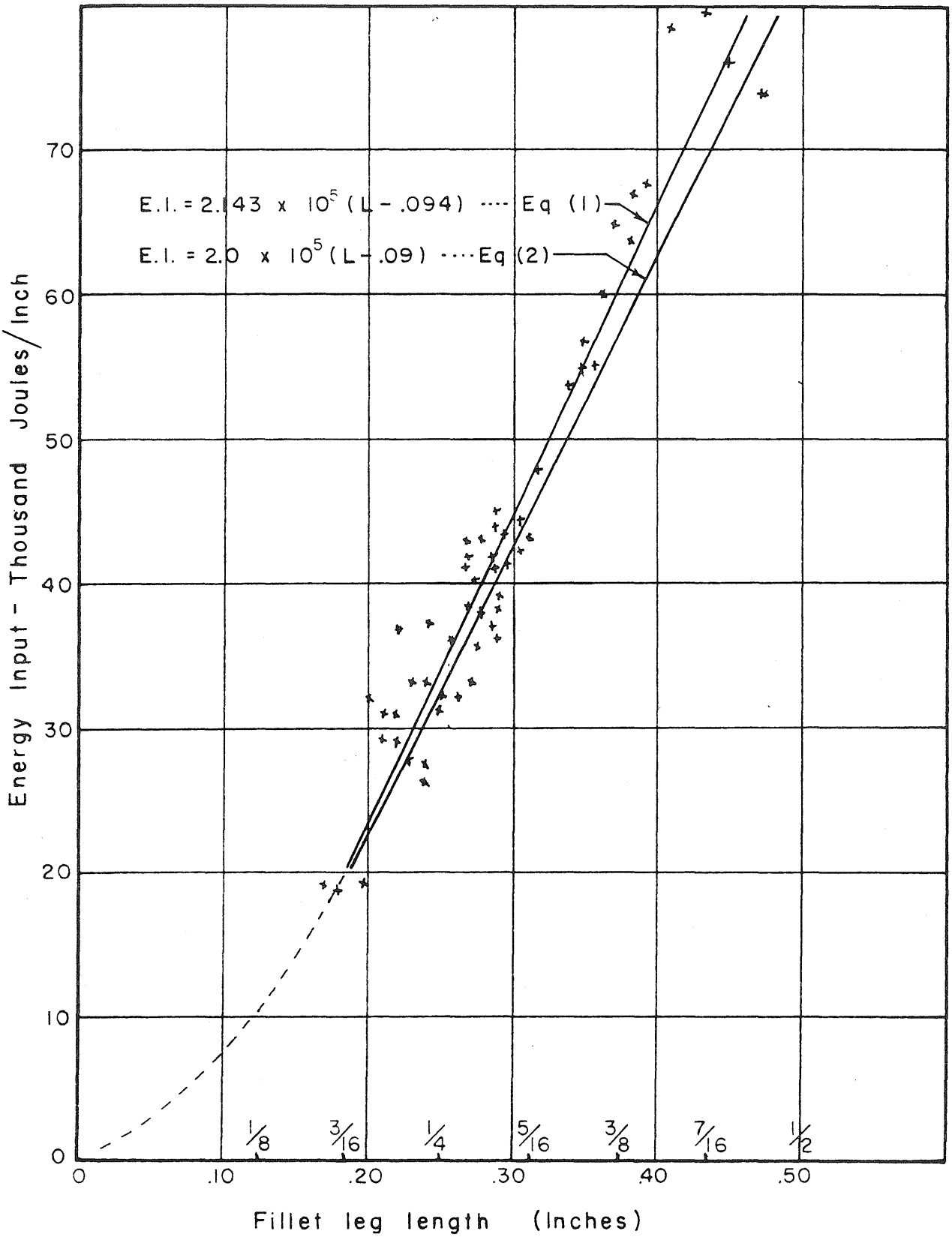

Fig. 15 Relationship Between Energy Input Per Inch and Fillet Leg Length

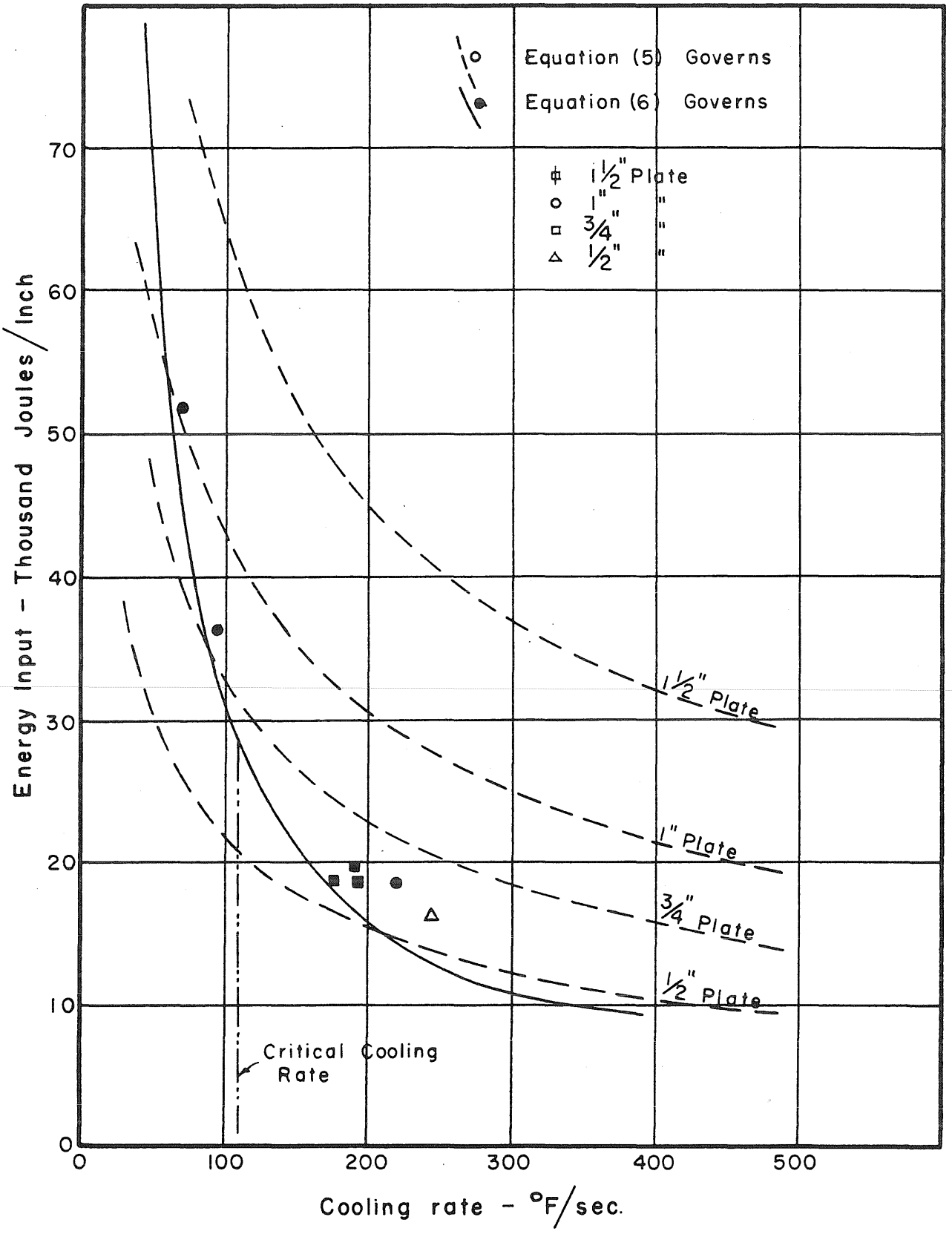

Fig. 16 Relationship Between Energy Input Per Inch and Cooling Rates at 750°F

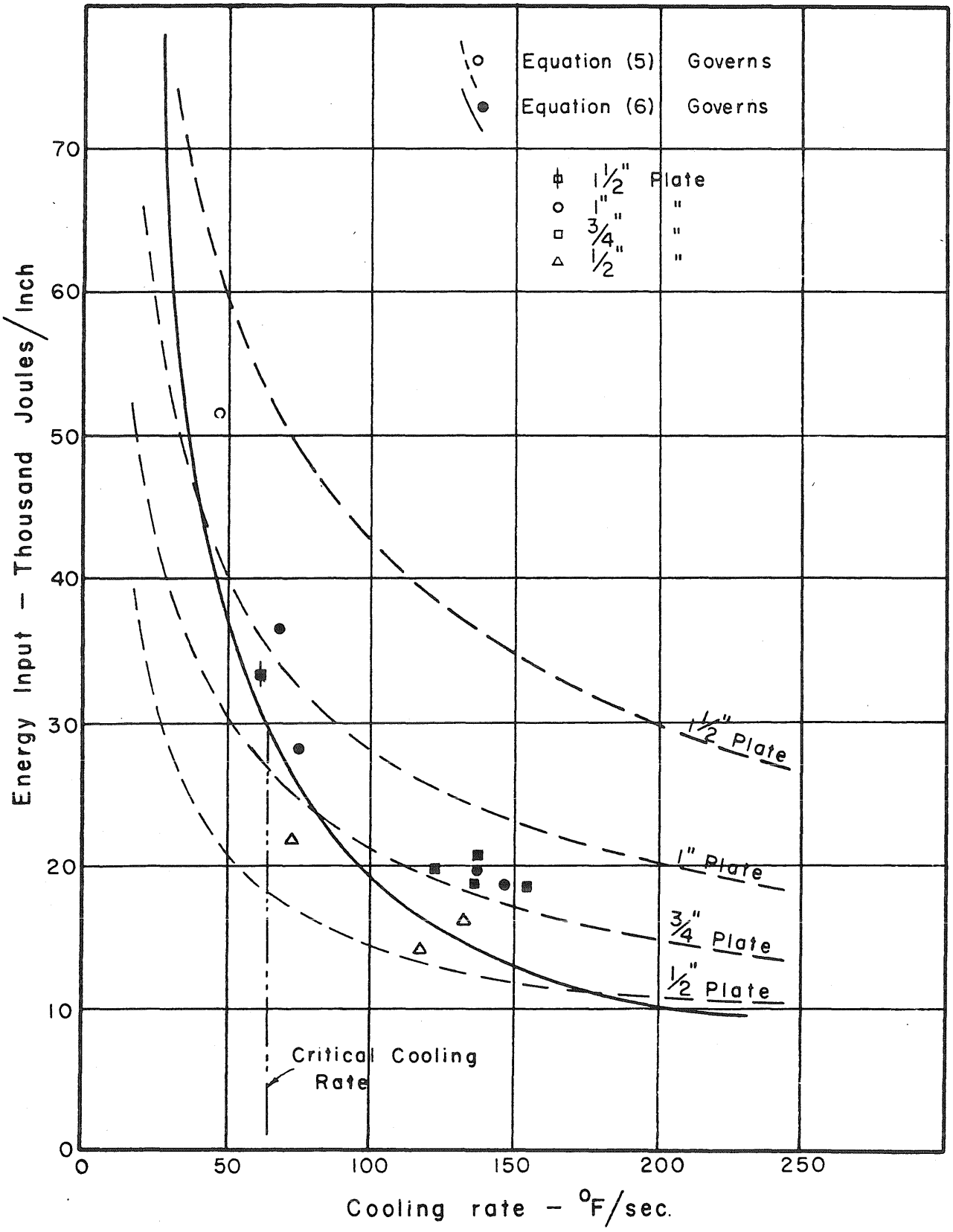

Fig. 17 Relationship Between Energy Input Per Inch and Cooling Rates at 572°F

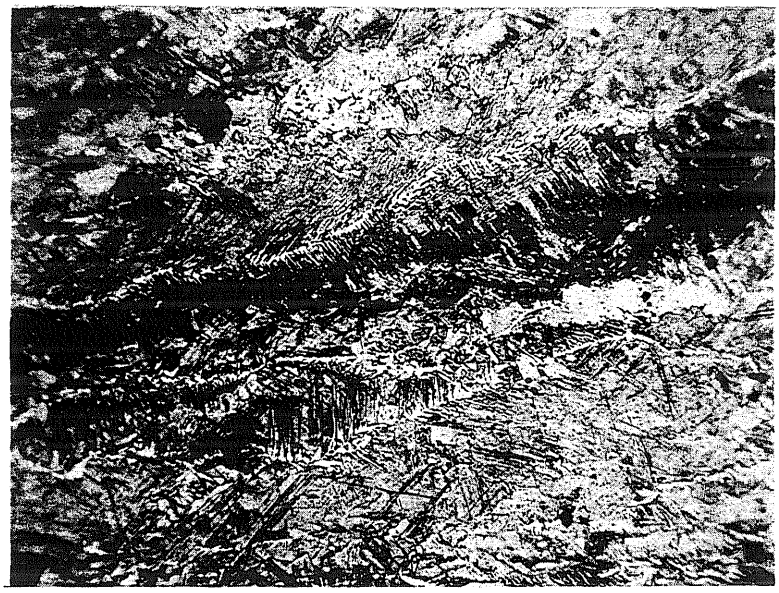

Fig. 18 Typical Weld Metal Micro-crack
Specimen C-12-1 Weld No. 2
(x 500)

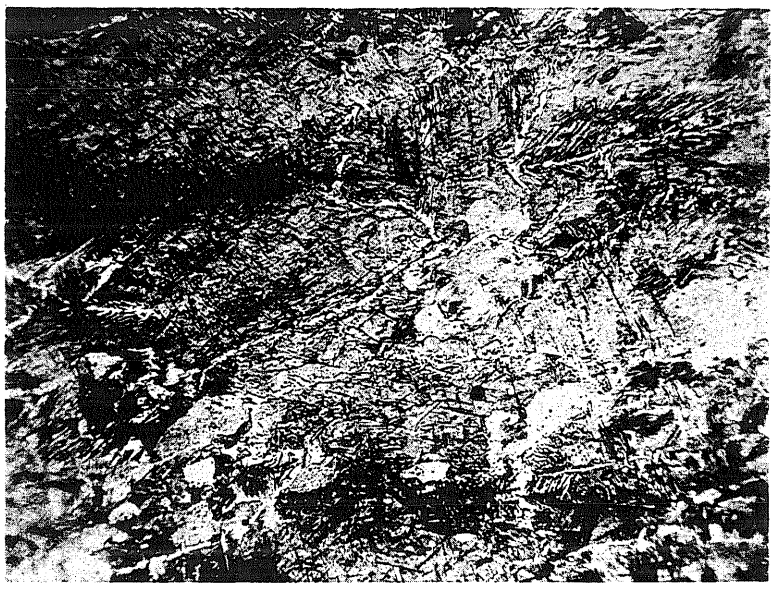

Fig. 19 Typical Weld Metal Micro-cracks
Specimen C-12-1 Weld No. 2
(x 500)

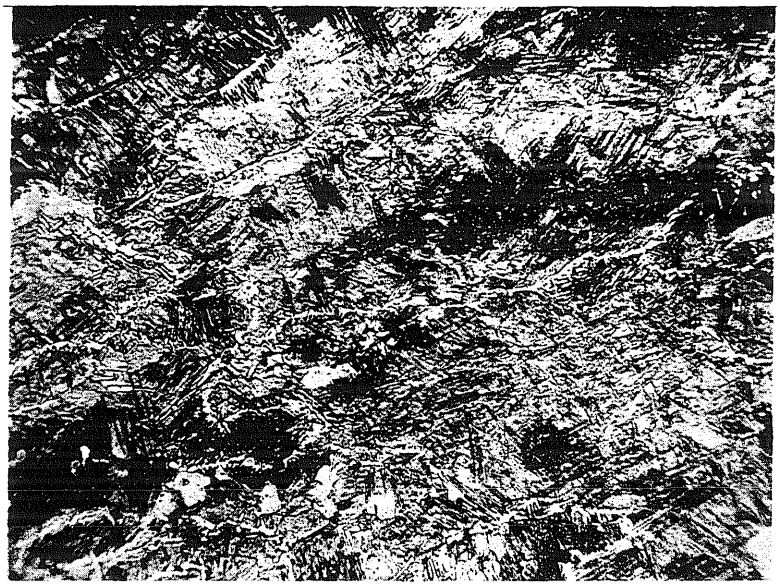

Fig. 20 Typical Weld Metal Micro-cracks
Specimen C-12-1 Weld No. 1
(x 500)

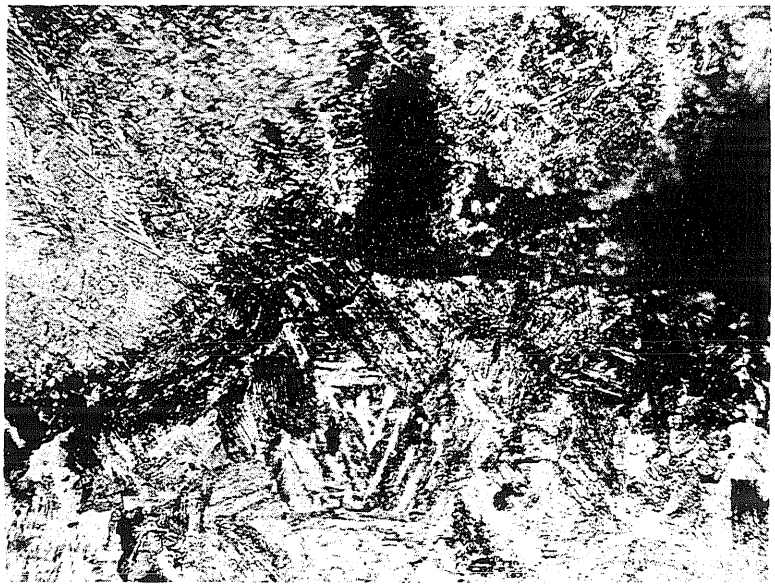

Fig. 21 Underbead Crack
Specimen B-1-2 Weld No. 1
(x 500)

Fig. 22 Crack That Propagated Into Heat Affected Zone
Specimen B-1-2 Weld No. 1
(x 500)

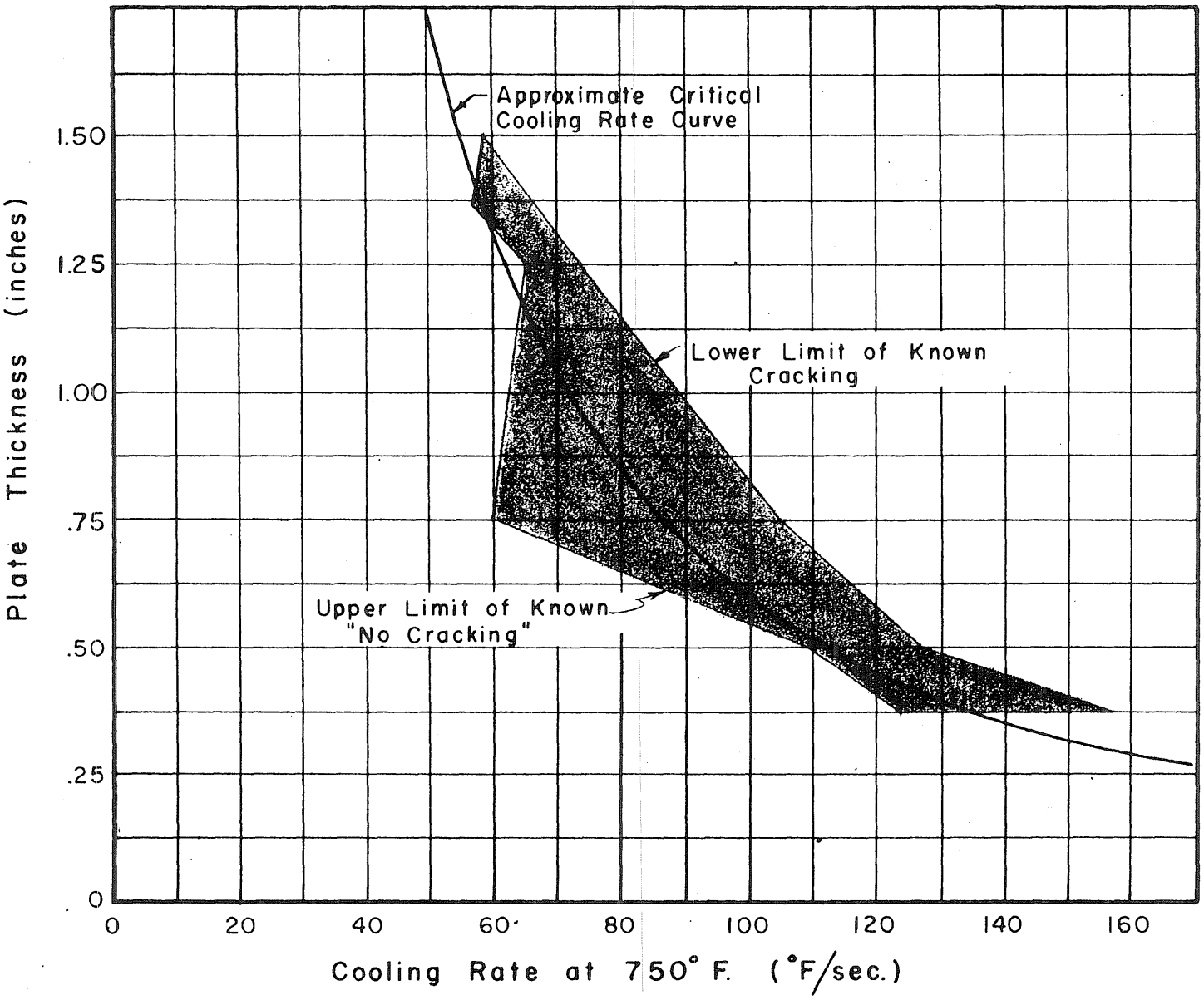

Fig.23 Plot of Plate Thickness vs. Cooling Rates Showing the Transition From Cracked to Uncracked Specimens

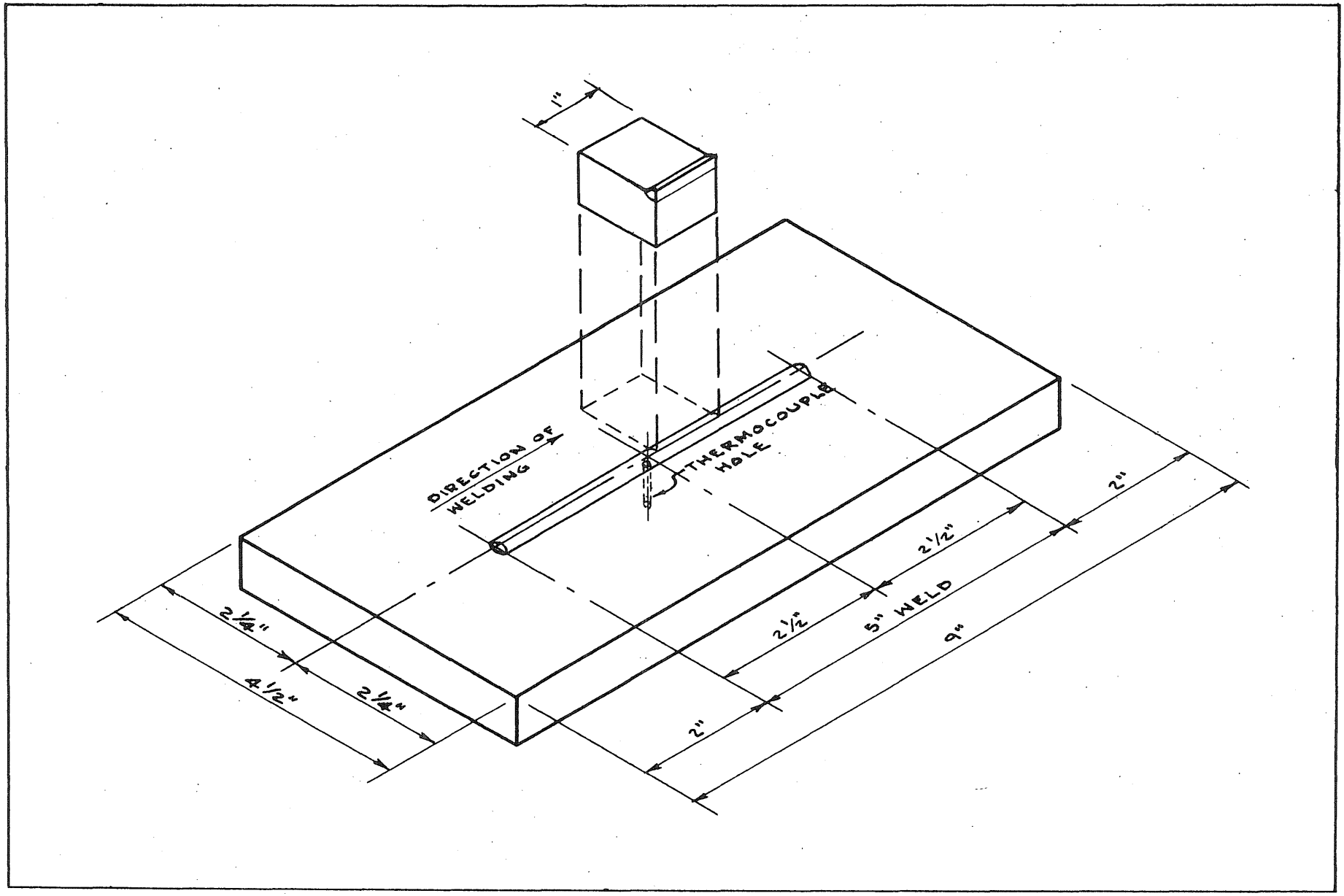

Fig. 24 Test Specimen and Section of Weld Examined for Cracking

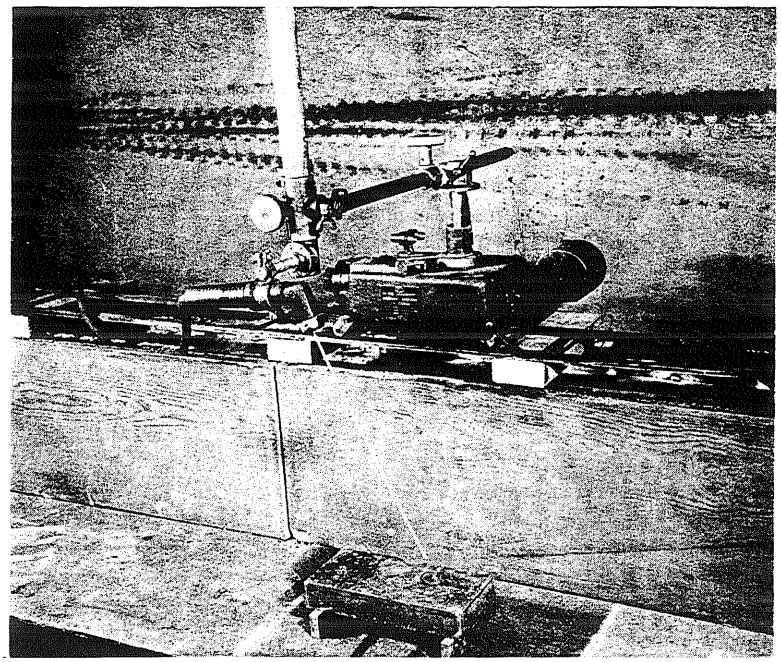

Fig. 25 Photograph Showing Semiautomatic Welding Equipment

Fig. 26 Crack in Weld Metal of Specimen P-3/8-3
Calculated Cooling Rate at 750°F = 187 °F/sec.
(x 500)

Fig. 27 Crack in Weld Metal of Specimen P-1/2-4
Calculated Cooling Rate at 750°F = 161 °F sec.
(x 500)

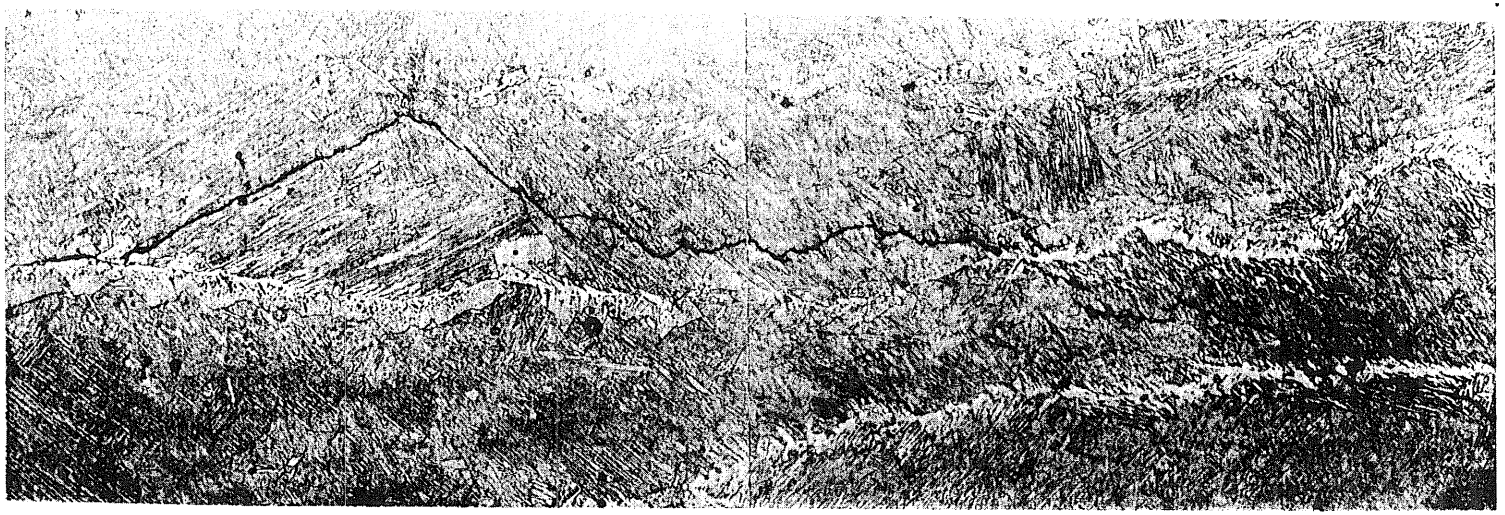

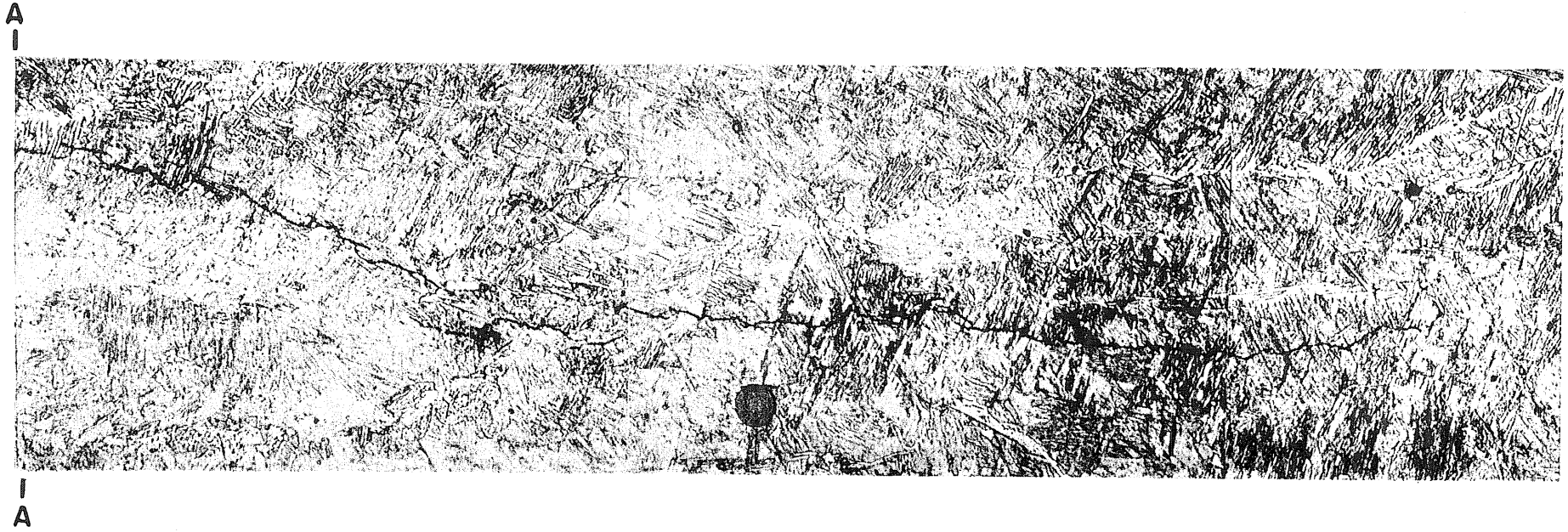

Fig. 28 Crack That Propagated into Heat Affected Zone, Specimen P-$\frac{3}{4}$-1
Calculated Cooling Rate at 750 °F = 118° F/sec.
(x 500)

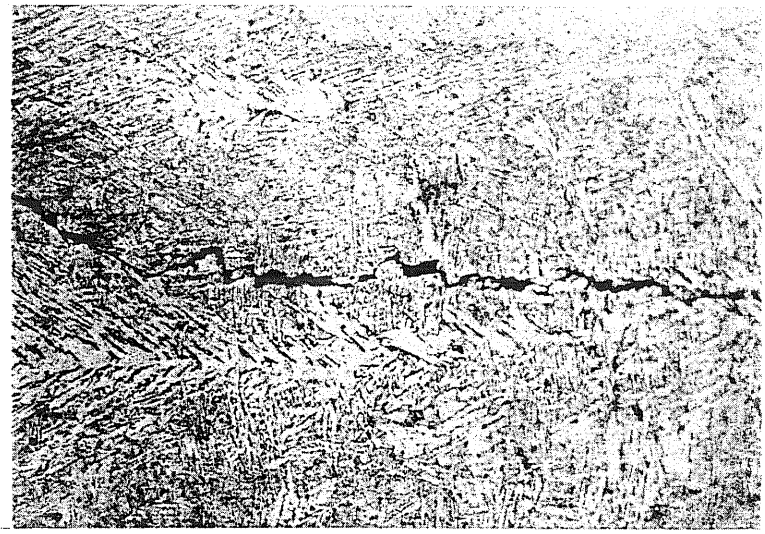

Fig. 29 Crack in Weld Metal of Specimen P-1 1/4-1
Calculated Cooling Rate at 750°F = 99.5°F/sec.
(x 500)

Fig. 30 Crack in Weld Metal of Specimen P-1 1/2-4
Calculated Cooling Rate at 750°F = 113.8°F/sec.
(x 500)

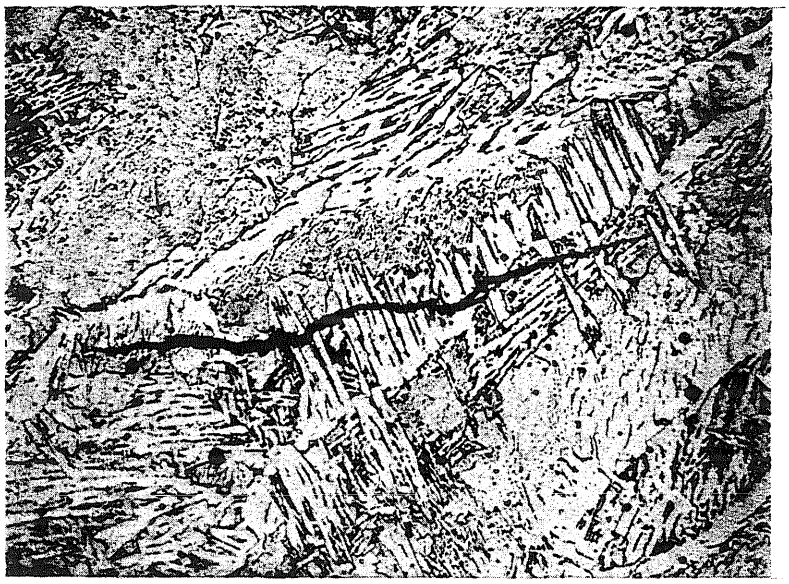

Fig. 31 Crack in Weld Metal of Specimen P-1½-3
Calculated Cooling Rate at 750 °F = 96.2 °F/sec.
(x 500)

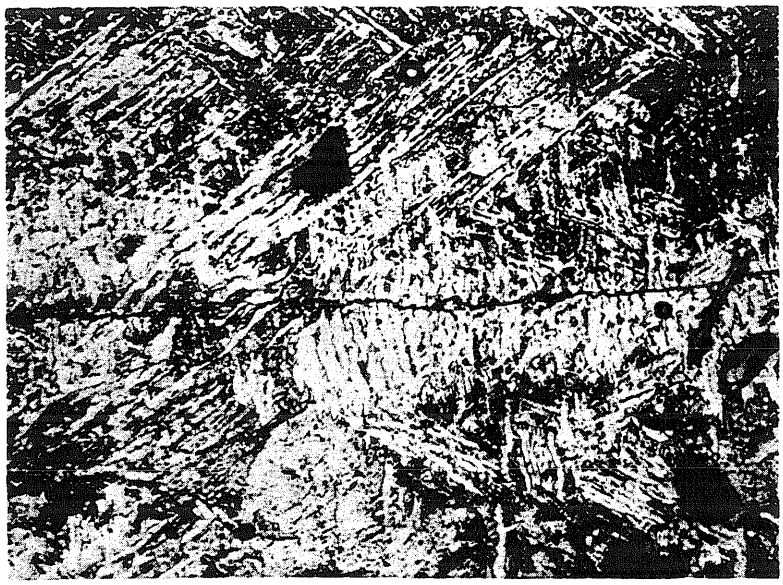

Fig. 32 Crack in Weld Metal of Specimen P-1½-2
Calculated Cooling Rate at 750 °F = 67.3 °F/sec.
(x 500)

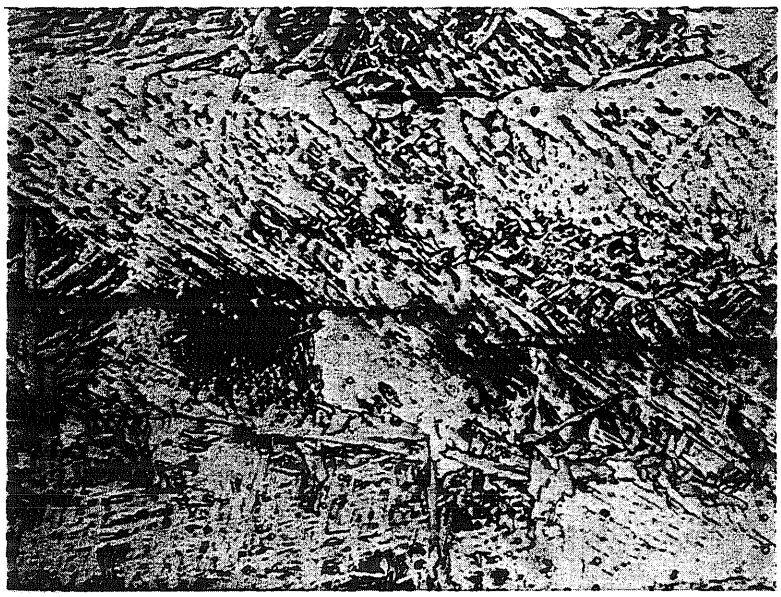

Fig. 33 Crack in Weld Metal of Specimen P-1½-1
Calculated Cooling Rate at 750°F = 58.6°F/sec.
(x 500)

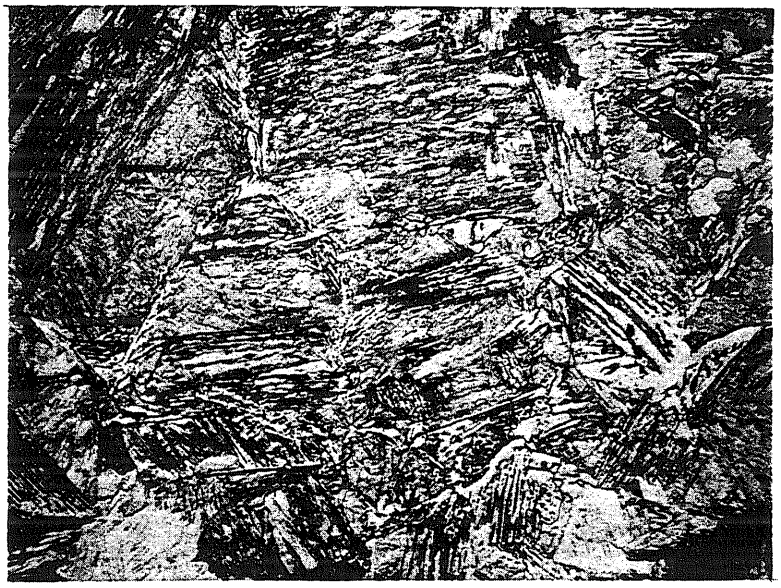

Fig. 34 Microstructure in Heat Affected Zone of Specimen P-½-3
Calculated Cooling Rate at 750 °F = 110 °F/sec.
(x 500)

Fig. 35 Photomicrograph Showing the Relative Size of Inclusions in Base Metal For Comparison With Microcracks.
Specimen P-1½-4 (x 500)

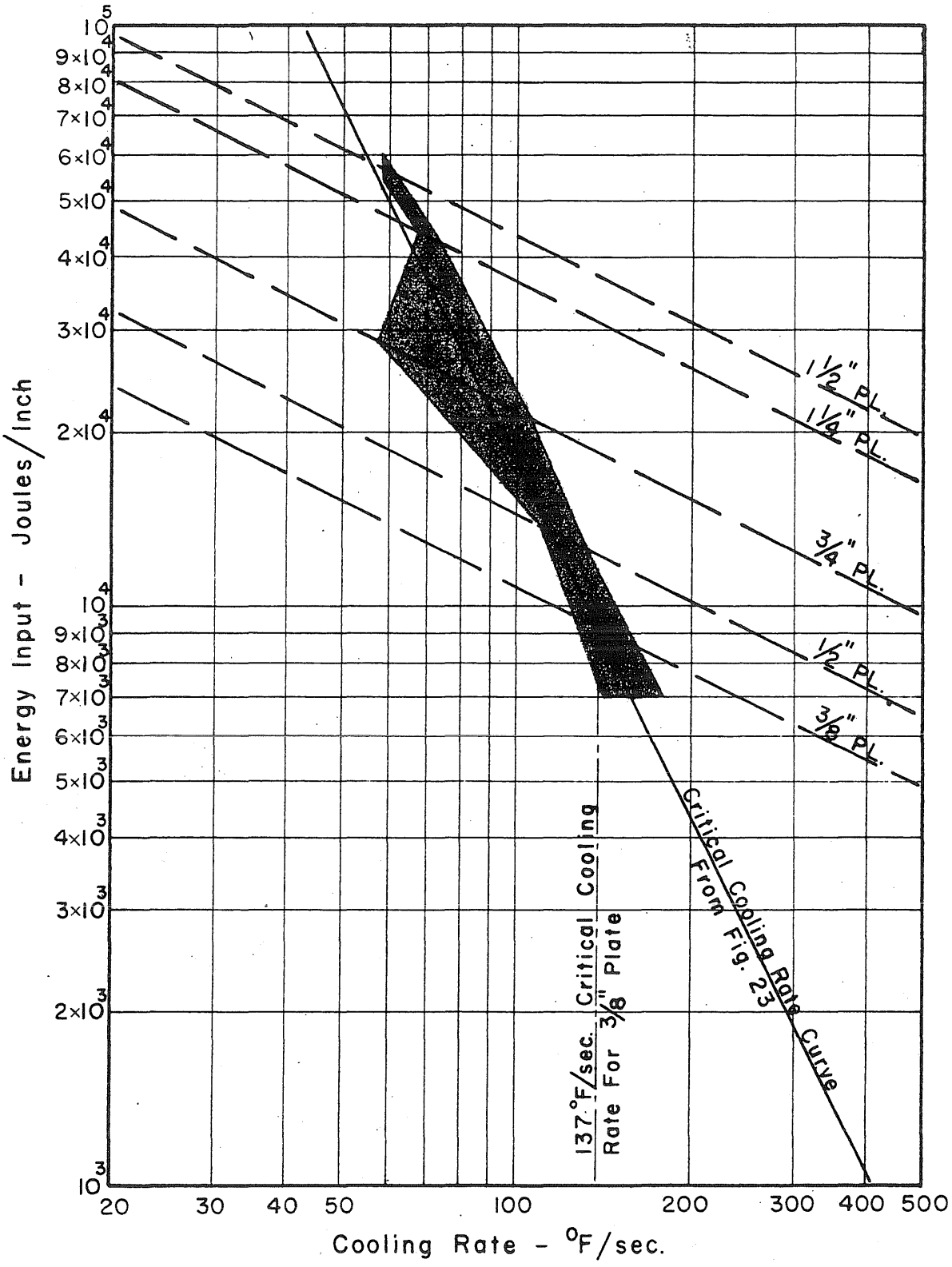

Fig. 36 Critical Cooling Rates at 750 °F For All Plate Thicknesses Tested

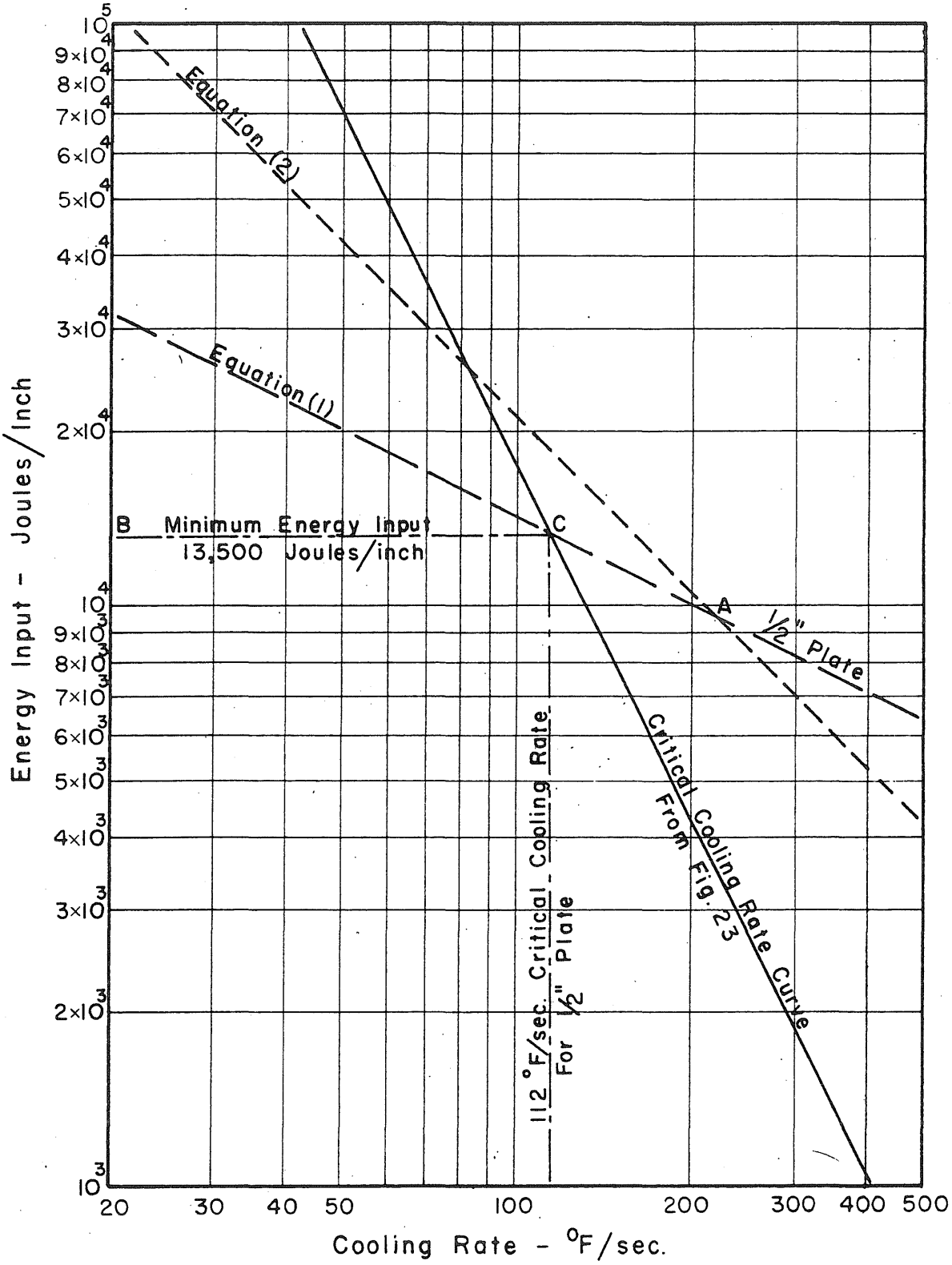

Fig. 37 Relationship Between Energy Input and Cooling Rates at 750° F For 1/2" Pl.

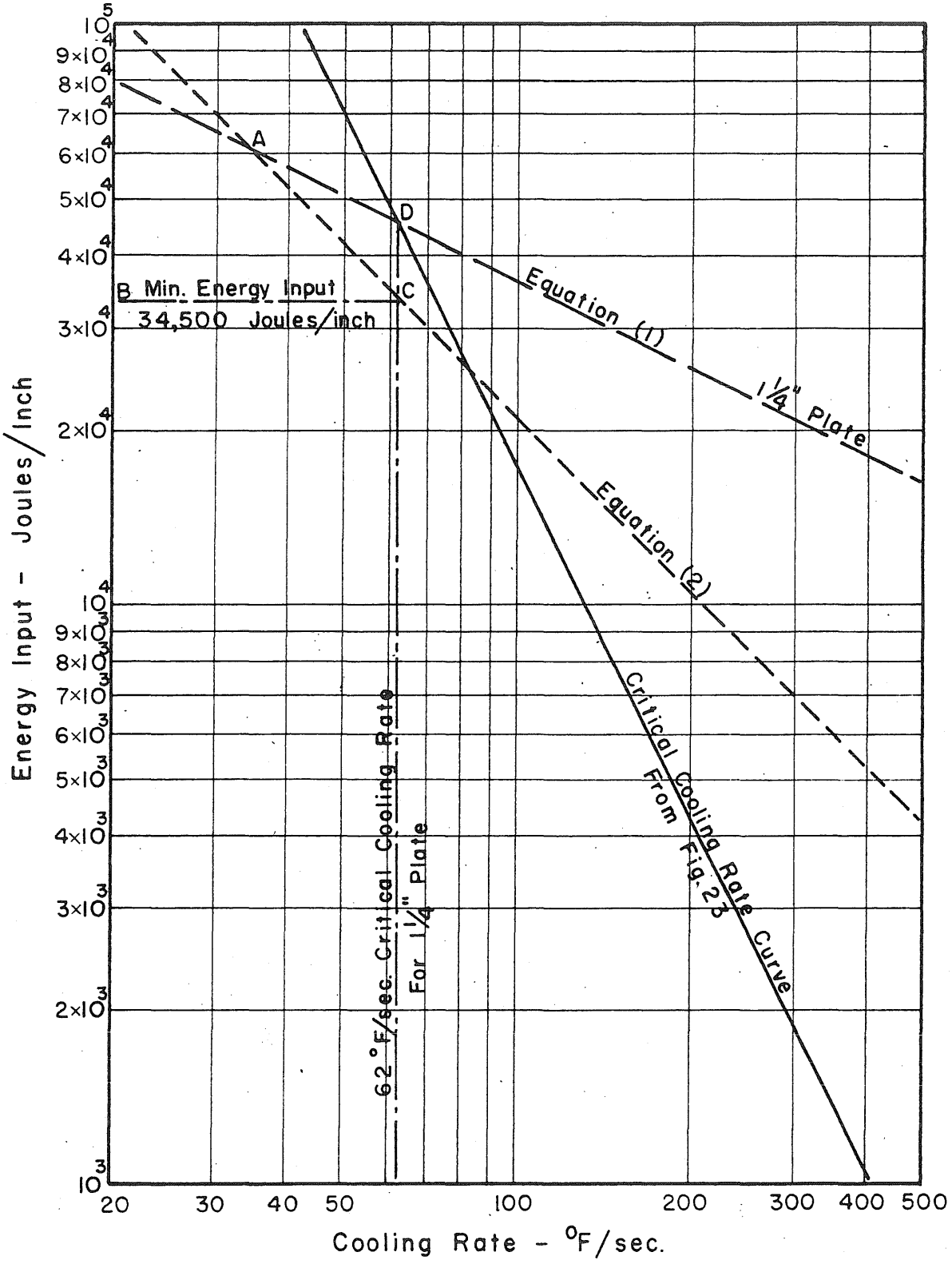

Fig. 38 Relationship Between Energy Input and Cooling Rates at 750 °F For 1¼" Pl.

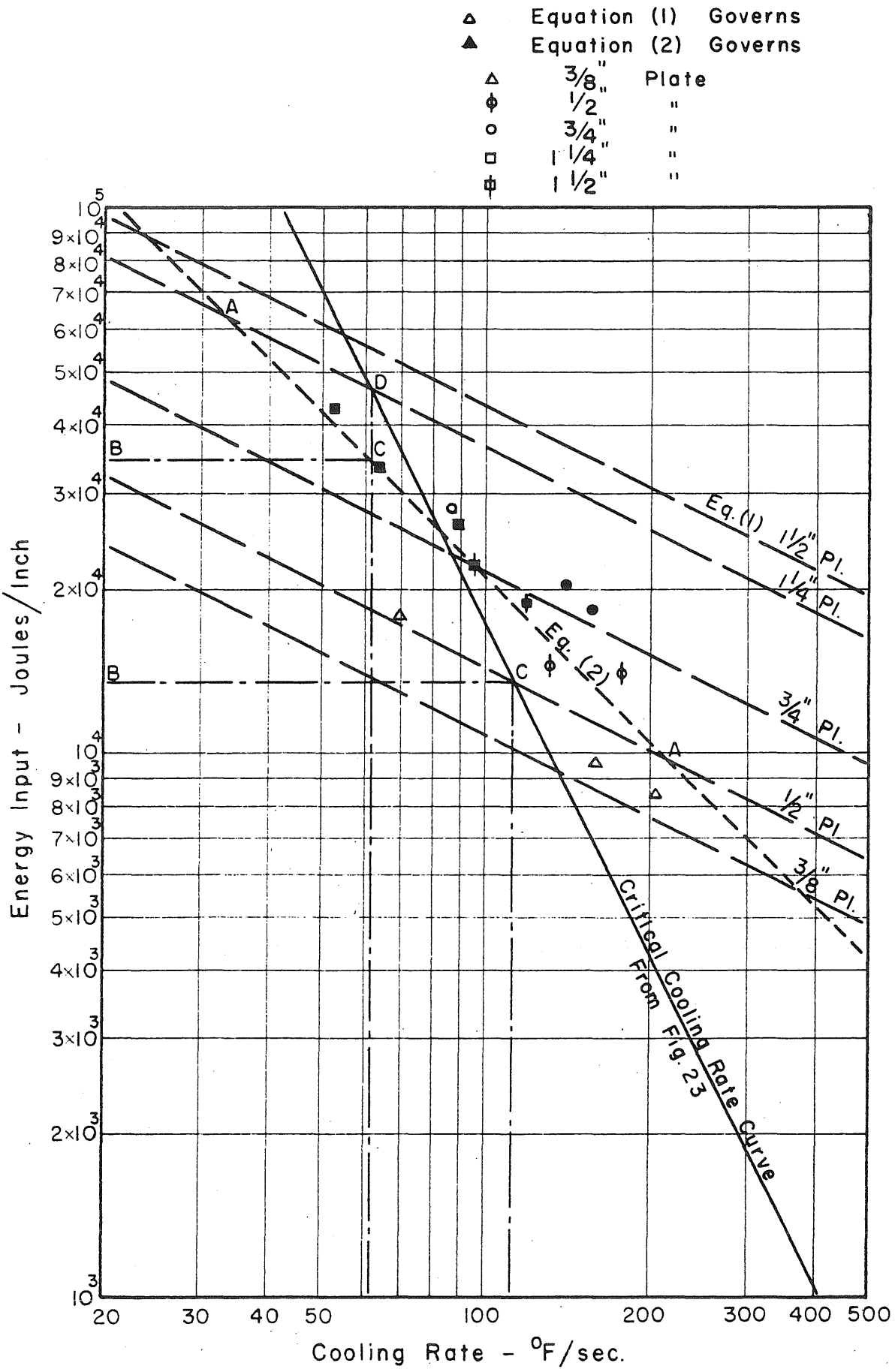

Fig.39 Relationship Between Energy Input and Cooling Rates at 750°F For All Plate Thicknesses Tested Using q = 80%

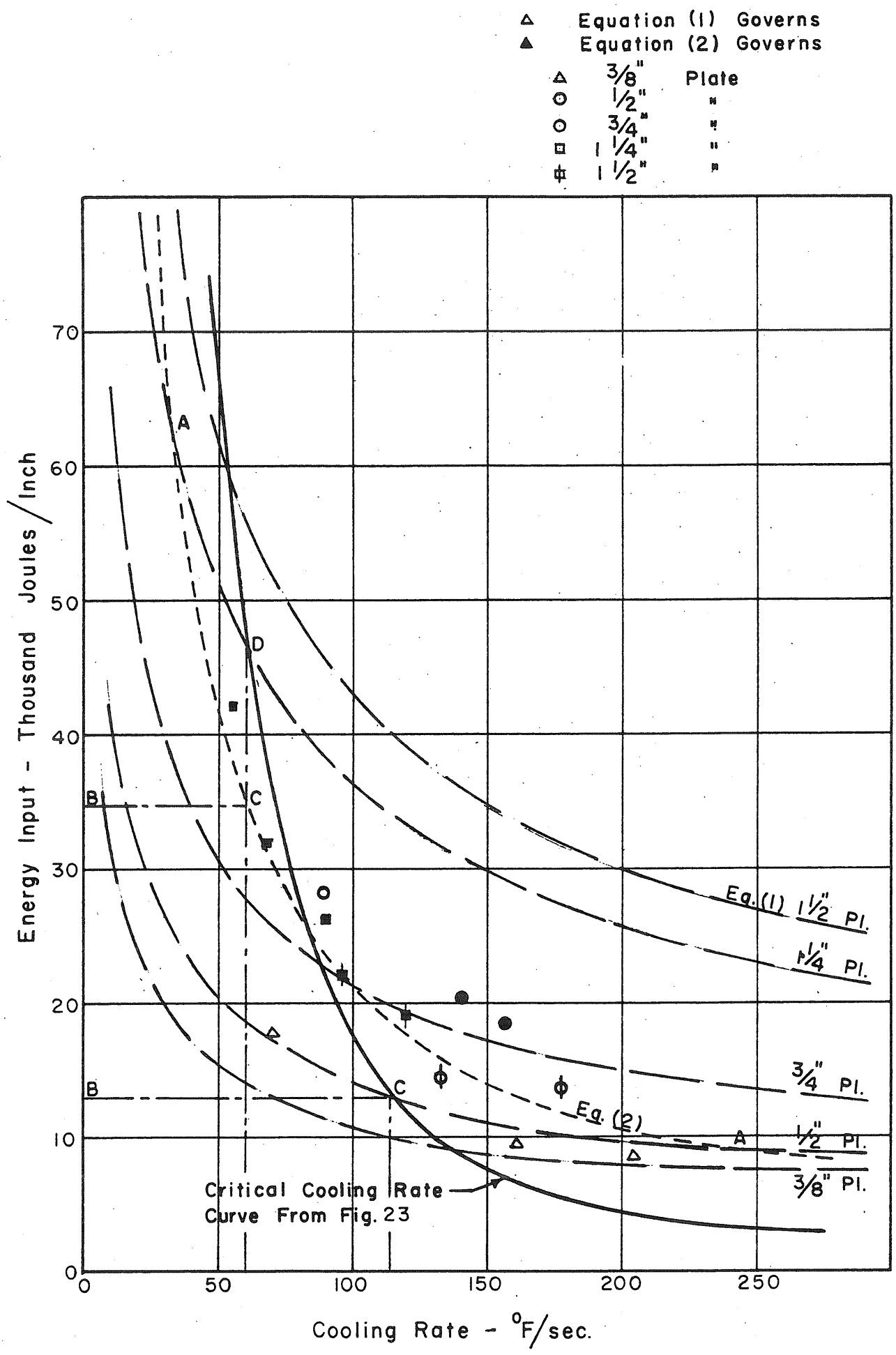

Fig.40 Relationship Between Energy Input and Cooling Rate at 750 °F For All Plate Thicknesses Tested Using a = 80 %

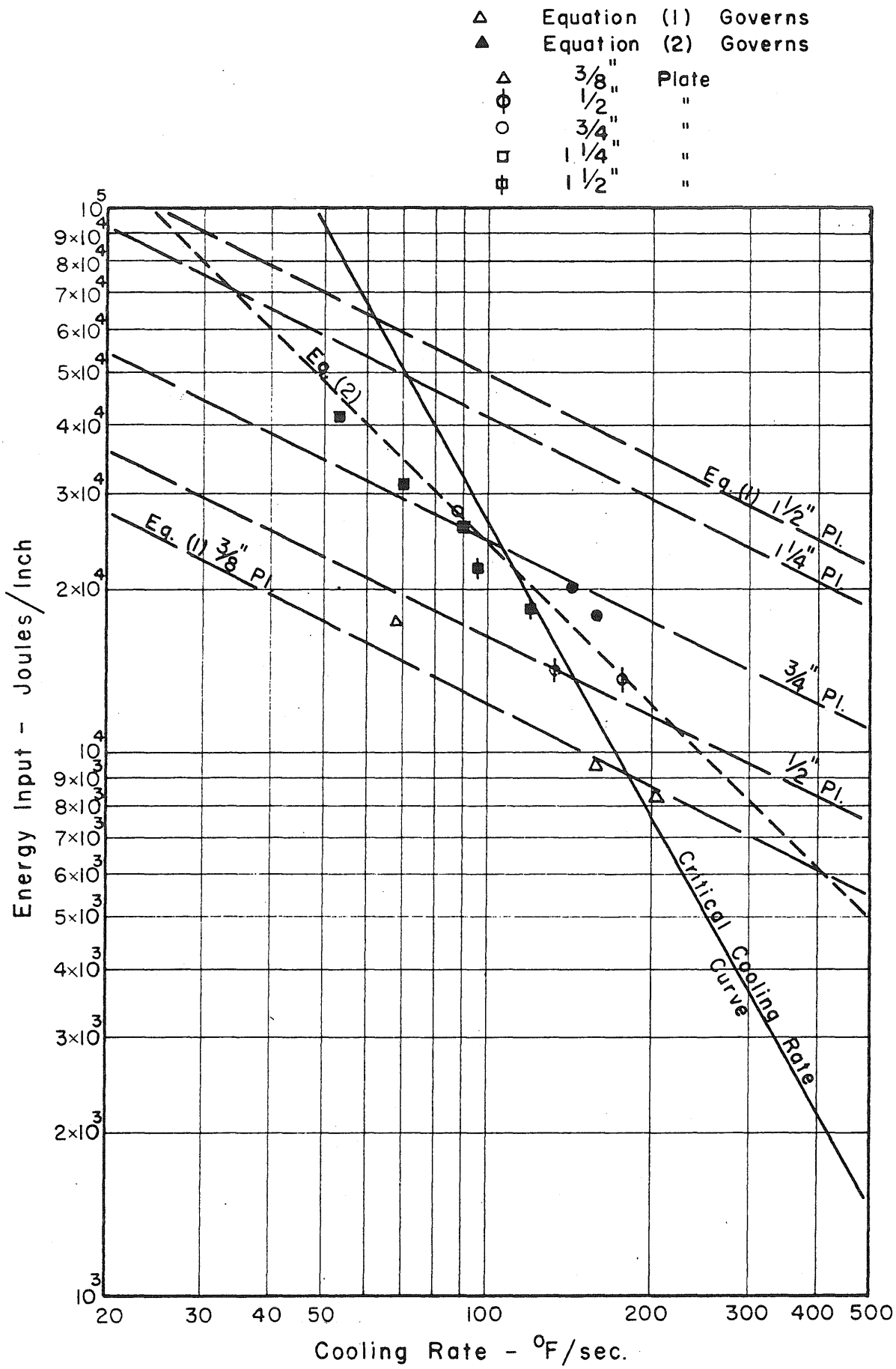

Fig.41 Relationship Between Energy Input and Cooling Rates at 750 °F For All Plate Thicknesses Tested Using q = 70 %